The Compressibility of Minimal Lattice Knots

E J Janse van Rensburg†§ and A Rechnitzer‡

†Department of Mathematics and Statistics, York University
Toronto, Ontario M3J 1P3, Canada
rensburg@yorku.ca
‡Department of Mathematics, The University of British Columbia
Vancouver V6T 1Z2, British Columbia , Canada
andrewr@math.ubc.ca

Abstract. The (isothermic) compressibility of lattice knots can be examined as a model of the effects of topology and geometry on the compressibility of ring polymers. In this paper, the compressibility of minimal length lattice knots in the simple cubic, face centered cubic and body centered cubic lattices are determined. Our results show that the compressibility is generally not monotonic, but in some cases increases with pressure. Differences of the compressibility for different knot types show that topology is a factor determining the compressibility of a lattice knot, and differences between the three lattices show that compressibility is also a function of geometry.

PACS numbers: 02.50.Ng, 02.70.Uu, 05.10.Ln, 36.20,Ey, 61.41.+e, 64.60.De, 89.75.Da

AMS classification scheme numbers: 82B41, 82B80

§ To whom correspondence should be addressed (rensburg@yorku.ca)

1. Introduction

The compressibility of polymer colloids, melts, and also of biopolymers, is an important physical property which affects rheology and other physical properties [20, 28]. The compressibility of linear polymers is monotonic non-increasing with pressure (see for example figure I in reference [20] or figures 15 and 16 in reference [28]), and typically approaches zero with increasing pressure.

In this paper, we will examine a model of the compressibility of tightly knotted ring polymers, where entanglements becomes an important factor in addition to geometry in determining the thermodynamic properties of the polymer. We do so by examining the compressibility of a lattice model of a knotted ring polymer.

Lattice polygons were introduced as a model of polymer entropy in ring polymers [9, 4]. In three dimensions a ring polymer may be knotted, and it is known that the topological properties of ring polymers have an important effect on entropy [8, 5]. Lattice knots are now a standard model for the polymer entropy problem in knotted ring polymers [22, 26, 10] and these objects have been the subject of numerous studies over the last two decades [19, 12, 27, 21, 11, 18, 25, 23]. One of the advantages in models of lattice knots is that they are effective numerical models of simulating the effects of topological constraints (knotting) on the properties of ring polymers, and although one may not obtain direct quantitative results for real ring polymers, qualitative results may be examined to gain insight into the physical properties of ring polymers generally.

The entropy of a ring polymer depends on its length (number of monomers) and on knots along the backbone of the polymer. Ring polymers which are too short cannot accommodate a knot, and one expect for each knot type there to be a minimal length which will allow the knot to be realised in the polymer. This situation is modeled by minimal length lattice knots [6, 7], which are idealised models of knotted ring polymers of minimal length (or equivalently, maximal thickness).

Examples of minimal length lattice knot in the simple cubic, face centered cubic, and body centered cubic lattices are illustrated in figure 1.

Figure 1. Examples of minimal length lattice trefoils (knot type 3_1^+ in the standard knot tables [3]) in three dimensional cubic lattices. These are embeddings in the simple cubic lattice (left), the face centered cubic lattice (middle), and the body centered cubic lattice (right).

Minimal length embeddings of lattice knots have residual conformational entropy (in addition to entropic contributions from translational and rotational degrees of freedom). For example, it is known that there are 75 distinct symmetry classes of

right handed lattice trefoil knots, which expand to 1664 distinct polygons when one accounts for rotational degrees of freedom as well [25].

The residual conformational degrees of freedom of minimal length lattice knots may seem a surprising feature of these models, and are known to be very dependent on the particular lattice [16]. However, minimal length ring polymers will similarly have some residual conformational degrees of freedom, even if tightly knotted. This would be because the discrete values of angles between adjacent bonds joining the monomers will admit different local geometric arrangements in the embedding of the polymer in free space. These arrangements will contribute to the entropy of the polymer, which is generally a function of the local geometry of the bonding (bonding angles, bond lengths). It will also be a function of the knot type if the polymer is knotted. The overall topology of the knotted polymer will constrain the molecule even locally to entangle in particular ways to complete the knot, in particular when it has minimal length. This will determine in some measure the entropy of the polymer.

In other words, while the entropic properties of minimal length lattice polygons will not produce quantitative results of real minimal length knotted ring polymers due to essential differences between the geometry of the lattice and polymers in three space, lattice knots are nevertheless a useful model to examine the qualitative nature of the interplay between topology and entropy in ring polymers.

In this paper we examine the (isothermal) compressibility of lattice knots as a model of the effects of pressure and topology on tightly knotted polymers. The compressibility will be defined by assuming the lattice knot to be in a bath of solvent molecules which are excluded from a volume about the lattice knot. The response of the lattice knot to increasing pressure in the solvent will be determined, and its compressibility thus determined.

Our numerical approach will be to determine the compressibility from exact numerical data on minimal length lattice knots obtained by using the GAS-algorithm for lattice knots [14, 15]. An excluded volume containing the lattice knot will be defined, and changes in its mean size to an externally applied pressure will be used to calculate the compressibility of the lattice knot as it is compressed in this volume.

Our approach defines an internal space close to the polygon which excludes solvent molecules, and increasing the ambient pressure will then compress the containing volume and the lattice knot inside it. We shall define two different volumes for this purpose, the first will be the smallest rectangular box containing the polygon, and the second will be a more close fitting envelope which will be defined using slices defined by the two dimensional convex hulls of intersections of lattice knots with lattice planes. The second volume is not necessarily convex, and will in many cases be smaller than the convex hull of the polygon, which is much harder to determine. We shall repeat these calculations the three cubic lattices, namely the simple cubic lattice (SC), the face centered cubic lattice (FCC) and the body centered cubic lattice (BCC).

In virtually all cases the lattice knots will be found to be compressible in general. Moreover, the compressibility will be found to have complicated and unexpected dependence on the applied pressure in some knots types, even exhibiting increasing compressibility with increasing pressure for some range of the applied pressure. For example, the compressibility β of a lattice trefoil in a pressurised rectangular box in the simple cubic lattice is shown in figure 2. β increases with small pressure to a peak, it then declines, and reaches a local maximum at intermediate pressures before it decreases to zero with large pressures. This unusual shape for the (p, β) curve shows that lattice trefoils may become relatively softer with increasing pressure in some

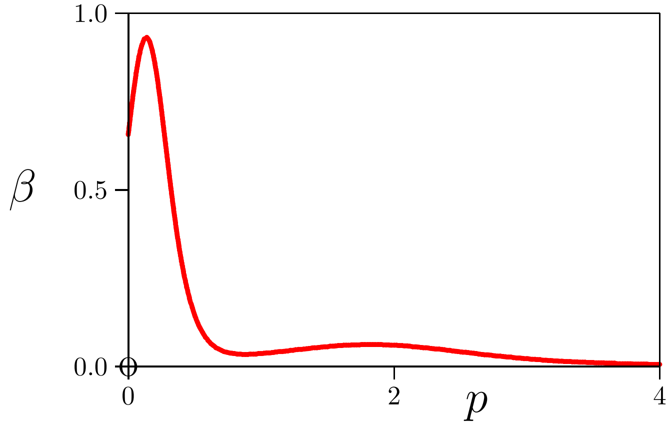

Figure 2. Compressibility of the minimal lattice knot of type 3_1^+ in the SC lattice.

pressure ranges – this kind of result would be dependent on both the lattice geometry and the topology of polygon, and so would not necessarily give a qualitative indication of the nature of real compressed ring polymers. However, the result suggests that this kind of behaviour is possible, as it is observed to some extend in all three the lattices we considered. Generally, however, different curves will be obtained for β in the other lattices.

We organised our paper as follows: In section 2 our methods and definitions are presented and explained. In section 3 we present results and discuss our findings. We conclude the paper in section 4.

2. The Compressibility of Minimal Length Lattice Knots

The SC lattice will be realised as $\mathbb{Z}^3$ with basis $\{(1,0,0),(0,1,0),(0,0,1)\}$ and edges of length 1. The FCC lattice has basis $\{(\pm1,\pm1,0),(\pm1,0,\pm1),(0,\pm1,\pm1)\}$ for all possible choices of the signs, and edges between adjacent vertices of length $\sqrt{2}$, while the BCC will have basis $\{(\pm1,\pm1,\pm1)\}$ for all possible choices of the signs, and edges of length $\sqrt{3}$.

Polygons in the SC, FCC and BCC lattices are sequences of vertices and edges $\{v_0, e_1, v_1, e_2, v_2, \ldots, v_{n-1}, e_n, v_n\}$ where $v_0 = v_n$ and all the vertices v_i are distinct. Then end-vertices of edges e_i are v_{i-1} and v_i. The *length* if a polygon ω is the number of edges it contains, and the *chemical length* will be the length times the length of edges: For example, if a polygon has length n, then its chemical length in the SC lattice is n, in the FCC lattice is $n\sqrt{2}$ and in the BCC lattice is $n\sqrt{3}$ since edges have length 1, $\sqrt{2}$ and $\sqrt{3}$ in the SC, FCC and BCC lattices respectively. In other words, the chemical length coincides with the geometric length of the polygons.

Polygons will be considered to be identical if one is a translate of the other. Define $\mathcal{P}_K$ to be the set of minimal length lattice polygons of knot type K and length n_K. The cardinality of $\mathcal{P}_K$ is the number of polygons of knot type K and minimal length, and this is denoted by $p_L(K) = |\mathcal{P}_K|$ in the lattice L. For example, $p_{SC}(0_1) = 3$, $p_{FCC}(0_1) = 8$ while $p_{BCC}(0_1) = 12$. The minimal lengths of the unknot in the SC lattice is 4, while in the FCC lattice it is 3 and in the BCC lattice it is 4.

In order to determine the compressibility of lattice knots, it is necessary to define

the volume they occupy. An upper bound on the excluded volume of a lattice knot is the minimal volume rectangular box with sides parallel to the X-, Y- and Z-axes containing it. A lower bound can be obtained by noting that a particular lattice knot ω should occupy at least the sites along its length, and also the intersection of the minimal rectangular box containing it with the union of the Wigner-Seitz cells along its length. This lower bound is perhaps too small, as interstitial space surrounded by vertices of the lattice knot should also be part of the excluded volume. Hence, we choose to require the excluded volume of a lattice knot to be a convex region containing the knot.

In the first instance, the smallest rectangular box in the lattice containing the lattice knot was taken as an excluded volume V_b about the knot. A second, smaller excluded volume V_e is defined by slicing the lattice knot with lattice planes, computing convex hulls in these planes, and then gluing them in slabs together to find a more tightly fitting volume about the lattice knot. We call this volume the *the averaged excluded volume* V_e of the lattice knot. A more careful definition is given below. In both cases we assume that solvent molecules pressurising the lattice knot is excluded from the excluded volume V_b and V_e, and increases in pressure in the solvent will pressurise the knot by exerting a pressure on the convex boundary of the volume about the lattice polygon.

Once the volumes containing lattice knots have been defined, they can be pressurized in these volumes and their compressibility determined. In this study we focus on the compressibility of lattice knots by using the minimal rectangular box and averaged excluded volume.

2.1. The rectangular box volume of lattice polygons

The volume of the smallest rectangular box with sides normal to the lattice axes containing a lattice knot is its *box volume* V_b. This volume is a large overestimate of the volume occupied by the polygon, since it is likely to include large spaces near the eight corners of the box. Observe that if V_C is the volume of the convex hull of a polygon, then in general $V_C \leq V_b$, although both volumes are minimal convex shapes containing the polygon.

Define $p_L(v;K)$ to be the number of minimal length lattice polygons in a lattice L, of knot type K, minimal box volume v. Then $\sum_v p_L(v;k) = p_L(K)$ is the total number of minimal length lattice polygons of knot type K.

One may check that $p_{SC}(0;0_1) = 3$ but $p_{FCC}(1;0_1) = 8$. However $p_{BCC}(8;0_1) = 6$ and $p_{BCC}(4;0_1) = 6$, since there are two classes of minimal length unknotted polygons in the BCC lattice, one class of 6 elements in a minimal rectangular box of dimensions $2 \times 2 \times 2$, and a second class of 6 elements in a minimal rectangular box of dimensions $2 \times 2 \times 1$.

2.2. The averaged excluded volume of lattice polygons

Let ω be a lattice knot and P_z be a lattice plane normal to the Z-axis. For some choices of P_z the intersection $\omega \cap P_z = Q_\omega$ is not empty but contains a subset of vertices from ω. Let C_z be the convex hull of the points in Q_ω, then C_z is a (geometric) two dimensional polygon in the plane P_z.

Suppose that the (integer) values of z giving a non-empty intersection Q_ω are $\{z_0, z_1, \ldots, z_m\}$ with $z_{i-1} + 1 = z_i$ for $i = 1, 2, \ldots, m$.

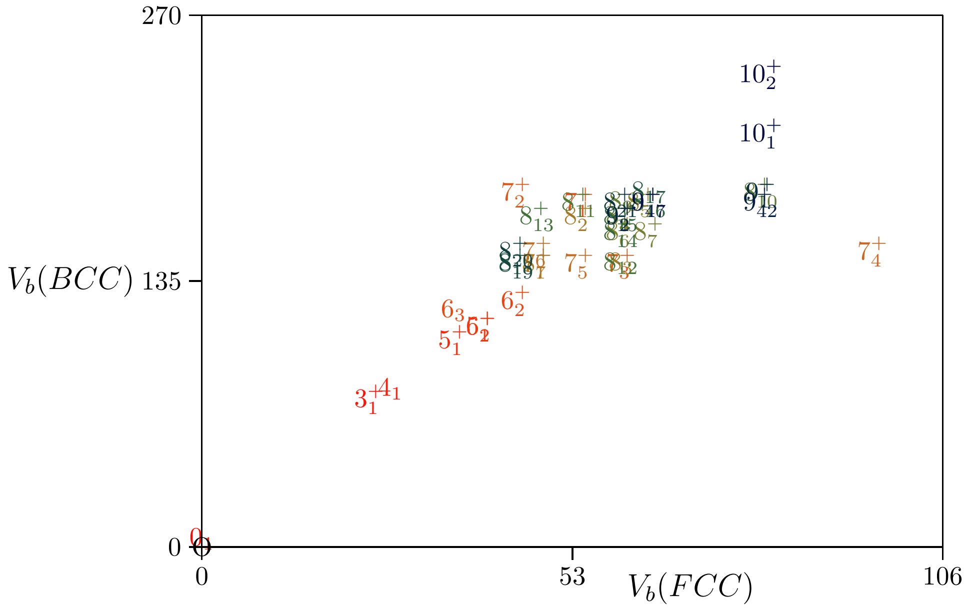

Figure 3. A scatter plot of the minimum rectangular box volumes V_b of knot types in the FCC and BCC. The points are contained in a narrow wedge, and the volumes are strongly correlated.

Define the slab $S_z = C_z \times [z-1/2, z+1/2]$ for each $z = z_i$ with $i = 1, 2, \ldots, m-1$. In addition, define $S_{z_0} = C_{z_0} \times [z_0, z_0 + 1/2]$ and $S_{z_m} = C_{z_m} \times [z_m - 1/2, z_m]$.

Define the volume V_z about ω by taking the union of these slabs:

$$V_z = \bigcup_{i=0}^{m} S_{z_i}.$$

Observe that the vertices of ω are contained in V_z, but that some edge may in fact be partially exposed. Since excluded volume effects in lattice polygons are defined in terms of vertices avoiding one another, we still consider V_z to constitute a volume containing ω, but it fits very tightly about the polygon in general.

Volumes V_x and V_y can be defined in this way by cutting ω by lattice planes normal to the X-axis or Y-axis instead. Taking the average gives the *average excluded volume* V_e of ω:

$$V_e = (V_x + V_y + V_z)/3.$$

Observed that $V_e \leq V_b$. One may also show that $V_e = 0$ for minimal length unknotted polygons in the SC, FCC and BCC lattices.

The values of V_e in the three lattices are strongly correlated across knot types. For example, in figure 4 a scatter plot of V_e in the SC and FCC is illustrated. The minimal values of V_e in the FCC and BCC are similarly plotted in figure 5 showing a strong correlation between the these minimal volumes in the FCC and BCC lattices.

The minimal values of V_b and V_e are strongly correlated for different knot types. For example, if the minimum value of V_b is relatively small for a knot type K, then so is the minimum value of V_e. In figure 6 the minimal values of (V_b, V_e) are illustrated in a scatter plot for the SC lattice.

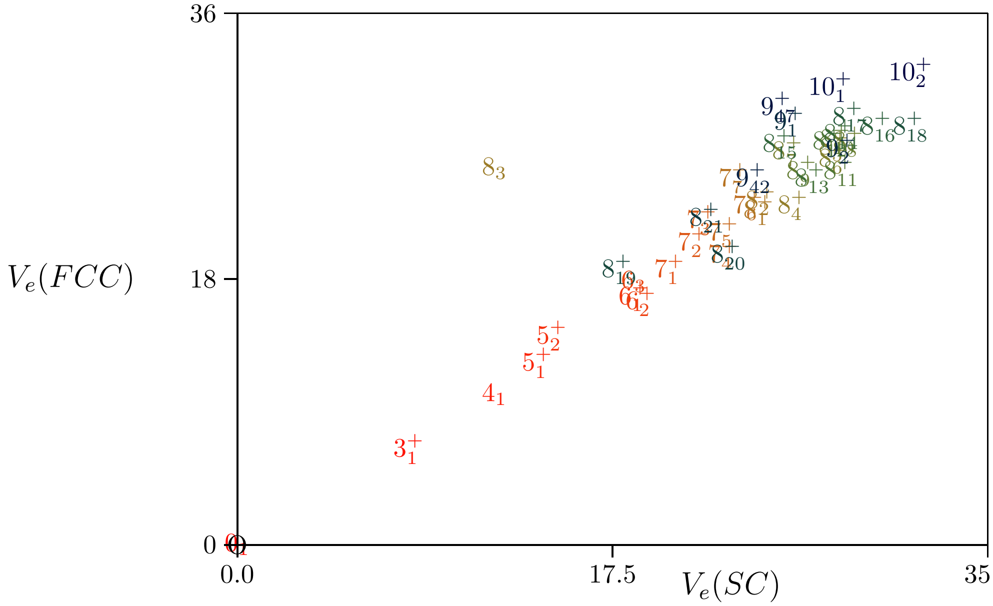

Figure 4. A scatter plot of the minimum average excluded volumes V_e of knot types in the SC and FCC. The points, with the exception of 8_3, are contained in a narrow wedge, and the volumes are strongly correlated.

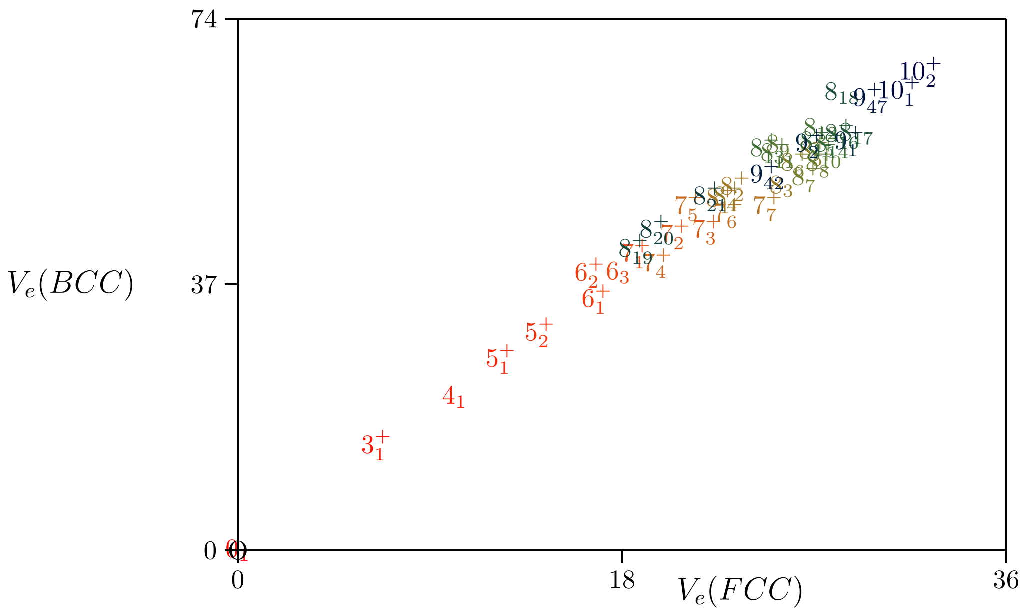

Figure 5. A scatter plot of the minimum average excluded volumes V_e of knot types in the FCC and BCC. The points are contained in a narrow wedge, and the volumes are strongly correlated.

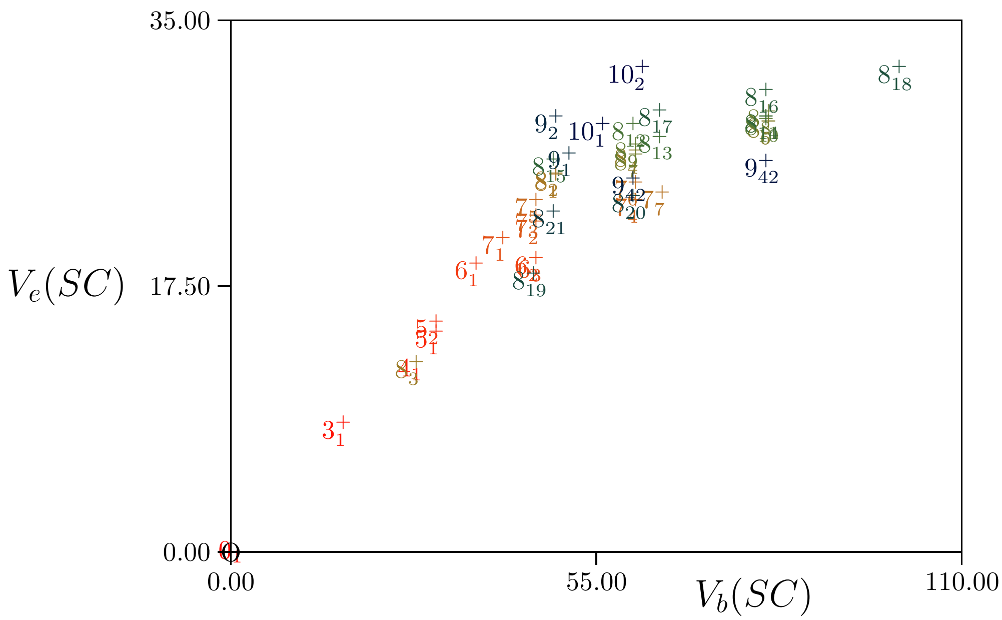

Figure 6. A scatter plot of $\min V_e(K)$ and $\min V_b(K)$ in the SC lattice for knot types K as indicated. The points are contained in a narrow wedge, and the volumes are strongly correlated.

2.3. The compressibility of minimal length lattice polygons

Consider a minimal lattice knot ω in a volume v_ω (which may be either the minimal box volume V_b, or the average excluded volume V_e). If the lattice knot is pressurized by an external pressure p, then its statistical mechanics properties will be described by its partition function, given by

$$\mathcal{Z}_L(K) = \sum_v p_L(v;K) e^{-p\,v}$$

where pressure and volume are in lattice units, and the Boltzmann factor is put equal to unity.

For example, the partition functions of minimal unknotted polygons with volumes V_b are given by

$$\mathcal{Z}_{SC}(0_1) = 3, \quad \mathcal{Z}_{FCC}(0_1) = 8e^{-p}, \quad \mathcal{Z}_{BCC}(0_1) = 6e^{-8p} + 6e^{-4p}.$$

If the volume V_e is used instead, then

$$\mathcal{Z}_{SC}(0_1) = 3, \quad \mathcal{Z}_{FCC}(0_1) = 8, \quad \mathcal{Z}_{BCC}(0_1) = 12.$$

The free energy of these models van be computed in the usual way: $\mathcal{F}_L(K) = -\log \mathcal{Z}_L(K)$. For example, the free energy of minimal length unknotted polygons in the BCC lattice in the rectangular box volume V_b is given by

$$\mathcal{F}_{BCC}(0_1) = -\log\left(6e^{-8p} + 6e^{-4p}\right). \tag{1}$$

This is explicitly dependent on p, and shows that pressurising minimal length unknotted BCC lattice polygons will lead to a response by adjusting the average equilibrium volume occupied by the polygon.

In the other cases the polygon will not respond to increasing pressure, and it is incompressible.

The average (equilibrium) volume occupied by a minimal length lattice knot at pressure p is obtained by

$$\langle V \rangle_L = \frac{\partial \mathcal{F}_L(K)}{\partial p}.$$

The compressibility of the body is defined by

$$\beta = -\frac{\partial \log \langle V \rangle_L}{\partial p},$$

and this definition shows that β is the fractional change in expected volume due to an increment in pressure. β is generally a function of temperature and pressure, and since temperature is fixed in this model, this is in particular the isothermal compressibility.

The average occupied rectangular box volume and compressibility of the minimal length unknot in the BCC lattice is

$$\langle V_b \rangle_{BCC} = \frac{4(1+2e^{-4p})}{1+e^{-4p}}.$$

When $p = 0$ this gives $\langle V_b \rangle_{BCC} = 6$ and if $p \to \infty$, then $\langle V_b \rangle_{BCC} = 4$. The compressibility can be computed directly:

$$\beta_{BCC}(0_1) = \frac{4e^{-4p}}{(1+e^{-4p})(1+2e^{-4p})}.$$

For the minimal length unknot in the other lattices, and also for the choice of V_e in all cases, the compressibility of the unknot is zero (that is, it is not compressible). The

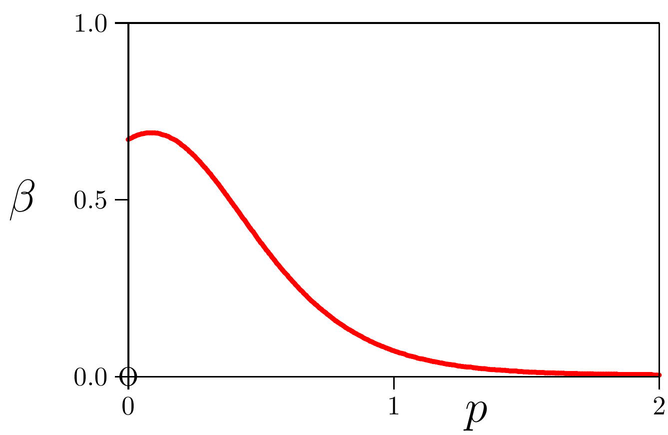

Figure 7. Compressibility of the BCC minimal lattice knot of type 0_1 in a rectangular box of volume V_b. Observe the global maximum at $p = 0.08664\ldots$ where $\beta = 0.68629\ldots$. If $p = 0$, then $\beta = 2/3$.

compressibility of the unknot in the BCC lattice with volume V_b is plotted in figure 7.

The minimum rectangular box volume containing a lattice knot K is its *minimal rectangular box volume* (in the case V_b), or its *minimal average excluded volume* (in the case of V_e). If a lattice knot is allowed to expand from its minimal volume to its equilibrium volume at zero pressure, there is a change in its free energy. The maximum amount of useful work that can be extracted from this expansion, if the

process is reversible, is given by the difference in free energies between the states at $p = 0$ (when the lattice knot is in an equilibrium state at zero pressure) and the state were the lattice knot is confined to its minimal volume.

Since the free energy of the unknot is independent of the pressure for the volume V_e, no useful work can be performed by a compressed unknot in any of the lattices. With the choice of volume V_b, the one exception is in the BCC lattice where $\mathcal{F}_{BCC}(0_1)$ is given by equation (1). Direct calculation shows that the maximum amount of work that can be performed by letting this polygon expand reversibly from its compressed state is $\mathcal{W}_{0_1} = \log 12 - \log 6 = \log 2$.

3. Compressibility of Lattice Knots: Numerical Results

3.1. GAS sampling of lattice knots

In this study we have sampled minimal length lattice polygons by implementing the GAS algorithm [14, 15]. The algorithm is implemented using a set of local elementary transitions (called "atmospheric moves" [13]) to sample along sequences of polygon conformations. The algorithm is a generalisation of the Rosenbluth algorithm [24], and is an approximate enumeration algorithm.

The GAS algorithm can be implemented in the SC lattice on polygons of given knot type K using the BFACF elementary moves [1, 2] to implement the atmospheric moves [15, 16]. This implementation is irreducible on classes of polygons of fixed knot type [17].

Atmospheric moves in the FCC and BCC lattices were defined in reference [16], and implemented using the GAS algorithm. As in the SC lattice, these atmospheric moves are irreducible on polygon classes of fixed knot type.

The implementation is described in detail in references [15, 16]). Polygons of fixed knot type were sampled along sequences, tracking their length and metric properties. Minimal length polygons were detected, classified by symmetry class, stored by hashing and written to disk for later analysis.

The GAS algorithm was implemented efficiently using hash coding which allowed elementary moves to be executed in $O(1)$ CPU time, independent of length. This efficiency allowed us to perform billions of iterations on knotted polygons in reasonable real time on desk top linux workstations. Simulations were performed by sampling up to 500 GAS sequences, each of length 10^7, to search and collect minimal length polygons. In most cases the minimal length polygons were detected fairly quickly, although some knot types prove a little harder and required more CPU time.

Data on minimal knots were collated and analysed separately. Minimal volumes V_b and V_e were computed for symmetry classes of the polygons and collected into expressions for the partition functions, from which free energies and compressibility were computed.

3.2. Compressibility of minimal length lattice knots in the SC lattice

The partition function of minimal length lattice knots with volumes given by V_b and up to 7 crossings are given in table 1. The partition functions of minimal lattice knots with volumes V_e (average excluded volumes) are listed in table 2 up to 5 crossing knots. These expression are typically far more complicated than those in table 1. By examining the partition functions in tables 1 and 2 the compressibility and other

Knot	$\mathcal{Z}_{SC}(p)$
0_1	3
3_1^+	$1220e^{-27p} + 432e^{-18p} + 12e^{-16p}$
4_1	$2784e^{-36p} + 864e^{-27p}$
5_1^+	$432e^{-48p} + 624e^{-36p} + 2160e^{-32p} + 120e^{-30p}$
5_2^+	$40536e^{-48p} + 4200e^{-45p} + 10560e^{-36p} + 2160e^{-30p}$
6_1^+	$2640e^{-48p} + 216e^{-45p} + 216e^{-36p}$
6_2^+	$7560e^{-64p} + 5256e^{-60p} + 3504e^{-48p} + 96e^{-45p}$
6_3	$2208e^{-64p} + 912e^{-48p} + 432e^{-45p}$
7_1^+	$288e^{-80p} + 252e^{-64p} + 11808e^{-60p} + 300e^{-54p} + 468e^{-48p} + 264e^{-45p} + 3600e^{-40p}$
7_2^+	$22404e^{-80p} + 2880e^{-75p} + 13032e^{-64p} + 85008e^{-60p} + 11712e^{-54p} + 22512e^{-48p} + 10632e^{-45p}$
7_3^+	$240e^{-45p}$
7_4^+	$24e^{-64p} + 60e^{-60p}$
7_5^+	$4392e^{-64p} + 216e^{-60p} + 96e^{-48p} + 24e^{-45p}$
7_6^+	$10368e^{-80p} + 4728e^{-64p} + 1920e^{-60p}$
7_7^+	$168e^{-80p} + 84e^{-64p}$

Table 1. Partition Functions: Minimal SC lattice knots in a Pressurized Rectangular Box.

properties of the minimal length lattice knots can be determined exactly.

3.2.1. Compressibility of 3_1^+ in the SC lattice: The compressibility of the trefoil knot displayed in figure 2 was obtained by choosing the volume V_b in the SC lattice. The partition function in this case is given by

$$\mathcal{Z}_{SC}(3_1^+) = 1220e^{-27p} + 432e^{-18p} + 12e^{-16p}. \tag{2}$$

The expected volume of the lattice knot at pressure p is

$$\langle V_b \rangle = \frac{3\left(2745e^{-27p} + 648e^{-18p} + 16e^{-16p}\right)}{305e^{-27p} + 108e^{-18p} + 3e^{-16\,p}}$$

and the compressibility is explicitly given by

$$\beta = \frac{889380e^{-45p} + 36905e^{-43p} + 432e^{-34p}}{(2745e^{-27p} + 648e^{-18p} + 16e^{-16p})\,(305e^{-27p} + 108e^{-18p} + 3e^{-16p})}.$$

Plotting this function for $p \in [0,4]$ gives the curve in figure 2.

The compressibility of 3_1^+ is not monotone with increasing p but first goes through a global maximum and then again later through a local maximum at higher pressure. Paradoxically, the lattice knot becomes "softer" when compressed for some ranges of the pressure, in the sense that the fractional decrease in volume increases with p in some instances. This effect is likely due to the choice of V_b as an enclosing volume – as the pressure increase, the lattice knot starts to explore conformations which expand into the corners of the containing box more frequently, with the result that there is still space to expand into and compensate for the increasing pressure. The maxima in figure 2 can be determined numerically. The global maximum is located at $p = 0.13557\ldots$ where $\beta = 0.92845\ldots$. The local maximum is located at $p = 1.82115\ldots$ where $\beta = 0.05888\ldots$. The compressibility at zero pressure is $\beta = 0.65347\ldots$.

Knot	$\mathcal{Z}_{SC}(p)$
0_1	3
3_1^+	$84e^{-32p/3} + 24e^{-65p/6} + 300e^{-10p} + 96e^{-61p/6} + 240e^{-59p/6} + 128e^{-21p/2} + 48e^{-28p/3}$ $+168e^{-31p/3} + 48e^{-19/2p} + 72e^{-29p/3} + 12e^{-11p} + 72e^{-103p/12} + 192e^{-53p/6} + 48e^{-26p/3}$ $+24e^{-35p/4} + 48e^{-17/2p} + 24e^{-25p/3} + 24e^{-101p/12} + 12e^{-8p}$
4_1	$48e^{-155p/12} + 48e^{-43p/3} + 192e^{-79p/6} + 96e^{-151p/12} + 96e^{-25p/2} + 96e^{-175p/12} + 96e^{-38p/3}$ $+96e^{-13p} + 192e^{-173p/12} + 144e^{-55p/4} + 192e^{-77p/6} + 288e^{-14p} + 48e^{-59p/4} + 96e^{-12p}$ $+48e^{-41p/3} + 144e^{-40p/3} + 96e^{-53p/4} + 96e^{-167p/12} + 432e^{-83p/6} + 192e^{-85p/6}$ $+48e^{-157p/12} + 192e^{-57p/4} + 240e^{-161p/12} + 192e^{-27p/2} + 240e^{-163p/12}$
5_1^+	$96e^{-29/2} + 48e^{-173p/12} + 240e^{-185p/12} + 264e^{-91p/6} + 144e^{-59p/4} + 72e^{-187p/12}$ $+192e^{-61p/4} + 264e^{-181p/12} + 120e^{-175p/12} + 120e^{-43p/3} + 96e^{-44p/3} + 288e^{-89p/6}$ $+264e^{-31p/2} + 204e^{-15p} + 276e^{-46p/3} + 144e^{-179p/12} + 252e^{-47p/3} + 168e^{-95p/6} + 12e^{-16p}$ $+24e^{-14p} + 48e^{-169p/12}$
5_2^+	$2496e^{-109p/6} + 792e^{-115p/6} + 72e^{-47p/3} + 48e^{-20p} + 48e^{-179p/12} + 192e^{-235p/12}$ $+912e^{-229p/12} + 1320e^{-71p/4} + 1536e^{-227p/12} + 24e^{-181p/12} + 504e^{33p/2} + 720e^{-77p/4}$ $+2232e^{-35p/2} + 600e^{-39p/2} + 1656e^{-209p/12} + 1440e^{-215p/12} + 72e^{-61p/4} + 1584e^{-113p/6}$ $+768e^{-67p/4} + 120e^{-46p/3} + 696e^{-205p/12} + 264e^{-187p/12} + 2088e^{-53p/3} + 384e^{-59p/3}$ $+1392e^{-103p/6} + 192e^{-119p/6} + 1152e^{-17p} + 456e^{-199p/12} + 408e^{-49p/3} + 2184e^{-56p/3}$ $+72e^{-15p} + 360e^{-63p/4} + 72e^{-185p/12} + 504e^{-65p/4} + 1608e^{-52p/3} + 1224e^{-211p/12}$ $+1728e^{-221p/12} + 216e^{-95p/6} + 3264e^{-107p/6} + 2496e^{-37p/2} + 384e^{-197p/12} + 120e^{-79p/4}$ $+1728e^{-223p/12} + 1056e^{-101p/6} + 2916e^{-18p} + 168e^{-191p/12} + 312e^{-97p/6} + 1200e^{-75p/4}$ $+1728e^{-73p/4} + 24e^{-59p/4} + 768e^{-203p/12} + 336e^{-193p/12} + 600e^{-50p/3} + 2712e^{-55p/3}$ $+24e^{-121p/6} + 1128e^{-58p/3} + 24e^{-44p/3} + 276e^{-16p} + 1224e^{-69p/4} + 96e^{-91p/6}$ $+120e^{-31p/2} + 1200e^{-217p/12} + 480e^{-233p/12} + 936e^{-19p}$

Table 2. Partition Functions: Minimal SC lattice knots in pressurized in their averaged excluded volumes.

These results should be compared when the SC lattice knot of type 3_1^+ is instead considered but in the more tightly containing average excluded volume V_e. In this case the partition function is given by

$$\begin{aligned}\mathcal{Z}_{SC}(3_1^+) = 84e^{-32p/3} &+ 24e^{-65p/6} + 300e^{-10p} + 96e^{-61p/6} \\ &+ 240e^{-59p/6} + 128e^{-21p/2} + 48e^{-28p/3} + 168e^{-31p/3} \\ &+ 48e^{-19/2p} + 72e^{-29p/3} + 12e^{-11p} + 72e^{-103p/12} \\ &+ 192e^{-53p/6} + 48e^{-26p/3} + 24e^{-35p/4} + 48e^{-17/2p} \\ &+ 24e^{-25p/3} + 24e^{-101p/12} + 12e^{-8p}. \end{aligned} \tag{3}$$

The compressibility can be determined in this model as above. It is plotted in figure 8. In this case one notes that the scale of the β-axis is an order of magnitude smaller than the case in figure 2. The pressure range on the X-axis is also expanded to larger pressure (up to $p = 16$ in this case, compared to $p = 4$ in figure 2). The qualitative shape of the curve is also slightly changed; there is still a global maximum at a non-zero value of p, but the secondary local maximum has disappeared. Nevertheless, the general shape of the curve is comparable to the curve in figure 2. The global maximum is at $p = 0.61046\ldots$ and where $\beta = 0.05907\ldots$.

The maximum amount of useful work that can be performed by letting a lattice knot type 3_1^+ expand from its minimal containing volume to its equilibrium at zero

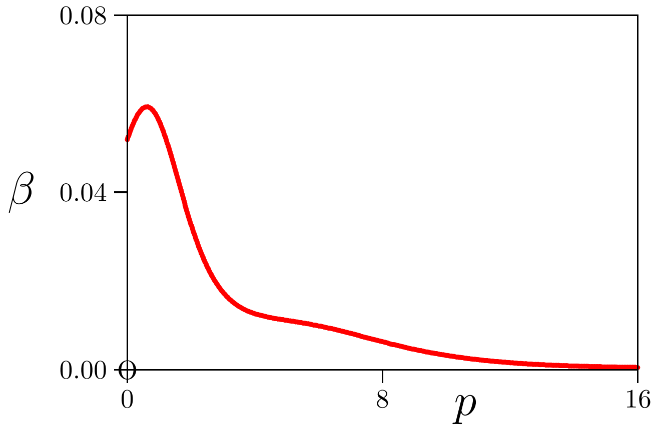

Figure 8. Compressibility of the minimal lattice knot of type 3_1^+ with volume V_e in the SC lattice.

pressure can be computed from the free energy of the model. If the volume V_b is used, then $\mathcal{F}_{SC}(3_1^+) = -\log \mathcal{Z}_{SC}(3_1^+)$ with the partition function given by equation (2).

By identifying the smallest value of V_b in equation (2), putting $p = 0$ and determining the free energy difference between the compressed and zero pressure state, it follows that the maximum amount of useful work is $\mathcal{W}_{3_1^+} = \log 1664 - \log 12 = \log(416/3) = 4.93207\ldots$. Interestingly, in this case the same result is obtained if one uses the average excluded volume instead.

3.2.2. Compressibility of 4_1*:* The compressibility of the figure eight knot 4_1 is illustrated in figure 9: In figure 9(a) the compressibility in a rectangular box volume V_b is shown, and in figure 9(b) the compressibility in an averaged excluded volume V_e is illustrated. Note the different scales on the axes of the two graphs. One

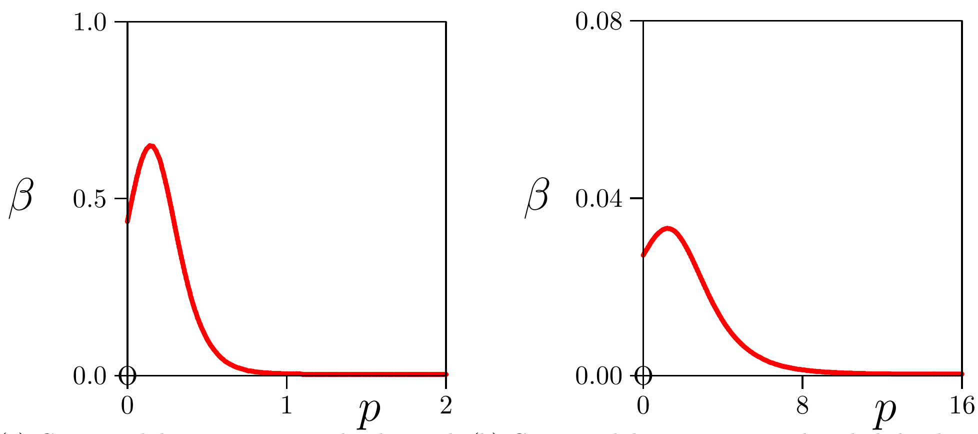

(a) Compressibility in a rectangular box volume V_b.

(b) Compressibility in a averaged excluded volume V_e.

Figure 9. Compressibility of the minimal lattice knots of type 4_1 in the SC lattice.

may similarly determine the maximum amount of useful work if the lattice knot is relaxed from its smallest containing volume to its state at zero pressure. If the volume V_b is used, then this is $\mathcal{W}_{4_1} = \log(38/9) = 1.44036\ldots$, and if V_e is used, then $\mathcal{W}_{4_1} = \log 38 = 3.63759\ldots$.

3.2.3. Compressibility of 5_1^+ and 5_2^+: The compressibilities of the two knots 5_1^+ and 5_2^+ are plotted in figure 10. For both choices of the volumes, the knot 5_2^+ is more compressible than 5_1^+. The generic shapes of the compressibility of 5_2^+ are similar for the two volumes, both cases having a global maximum away from zero pressure. In

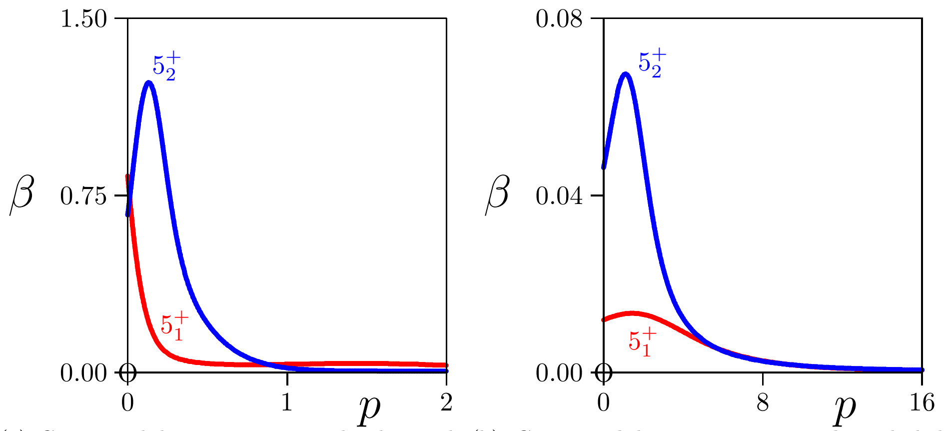

(a) Compressibility in a rectangular box volume V_b.

(b) Compressibility in a averaged excluded volume V_e.

Figure 10. Compressibility of the minimal lattice knots of types 5_1^+ and 5_2^+ in the SC lattice.

the case of 5_1^+ on the other hand, the global maximum in the compressibility is at zero pressure when the volume V_b is used, but it is at $p > 0$ when V_e is used. The maxima in figure 10(a) is at $p = 0$ ($\beta = 0.82695\ldots$) for 5_1^+ and $p = 0.13237\ldots$ ($\beta = 1.22294\ldots$) for 5_2^+. Observe that 5_1^+ has a local maximum at $p = 1.43622\ldots$ ($\beta = 0.03260\ldots$). In figure 10(b) the global maxima are located at $p = 1.43811\ldots$ ($\beta = 0.01308\ldots$) and $p = 1.11177\ldots$ ($\beta = 0.06718\ldots$) respectively.

The maximum amount of work that can be extracted from these two knot types were, for 5_1^+, $\mathcal{W}_{5_1^+} = \log(139/5) = 3.32504\ldots$ with volume V_b and $\mathcal{W}_{5_1^+} = \log 139 = 4.93447\ldots$ with volume V_e, and for 5_2^+, $\mathcal{W}_{5_2^+} = \log(133/5) = 3.28091\ldots$ with volume V_b and $\mathcal{W}_{5_2^+} = \log 2394 = 7.78072\ldots$ with volume V_e.

3.2.4. Compressibility of knots with 6 crossings: The compressibility of six crossing knots are displayed in figure 11. For both choices of V_b and V_e as containing volumes, the knot 6_3 were more compressible, and 6_1^+ least compressible.

In all three cases the maximal compressiblity were at non-zero pressure, and only in the case of 6_2^+ with volume V_b did we observe a local maximum in the compressibility at higher pressure, compared to the global maximum at low pressure. By using the volume V_b to measure compressibility, the (global) maxima in the compressibility were at $p = 0.22958\ldots$ where $\beta = 0.81816\ldots$ for 6_1^+, at $p = 0.09103\ldots$

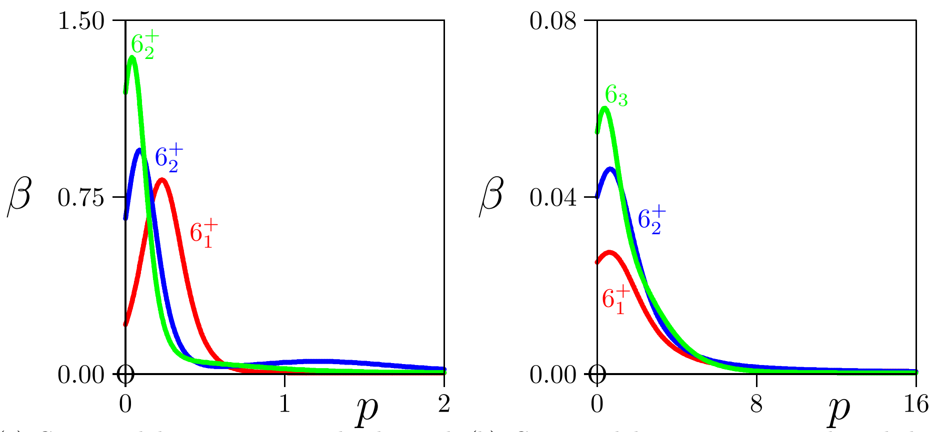

(a) Compressibility in a rectangular box volume V_b.

(b) Compressibility in a averaged excluded volume V_e.

Figure 11. Compressibility of the minimal lattice knots of types 6_1^+, 6_2^+ and 6_3 in the SC lattice.

where $\beta = 0.94524\ldots$ for 6_2^+ (with a local maximum at $p = 1.20977\ldots$ where $\beta = 0.04840\ldots$), and at $p = 0.04118\ldots$ where $\beta = 1.33719\ldots$ for 6_3.

The maximum amount for work that can be extracted from these knot types are $\mathcal{W}_{6_1^+} = \log(128/9) = 2.65481\ldots$, $\mathcal{W}_{6_2^+} = \log 171 = 5.14166\ldots$, and $\mathcal{W}_{6_3} = \log(74/9) = 2.10684\ldots$.

Using the volume V_e instead, one finds that global maxima at $p = 0.61767\ldots$ where $\beta = 0.02723\ldots$ for 6_1^+, at $p = 0.66097\ldots$ where $\beta = 0.04609\ldots$ for 6_2^+, and at $p = 0.37398\ldots$ where $\beta = 0.05988\ldots$ for 6_3.

The maximum amount for work that can be extracted from these knot types are $\mathcal{W}_{6_1^+} = \log 256 = 5.54517\ldots$, $\mathcal{W}_{6_2^+} = \log(36/19) = 6.52795\ldots$, and $\mathcal{W}_{6_3} = \log 74 = 4.30406\ldots$.

3.2.5. Compressibility of knots with 7 or more crossings: The compressibilities of 7 and 8 crossings knots for the choice V_b are summarized in table 3. Several minimal lattice knots in table 3 are incompressible, for example 0_1, 7_3^+, 8_5^+, 8_6^+ and so on. The largest compressibility at zero pressure is for the knot 8_3, and this is also the largest compressibility overall in the table. In this table the appearance of a local maximum in the compressibility, as seen for the trefoil in figure 2, for example, appears to be the exception, rather than the rule. Only the knot types 3_1^+, 5_1^+, 6_2^+, 9_2^+ and 10_1^+ have local maxima in their compressibility when pressurized in a rectangular box. Most knot types have maximum useful work between 0 and 3 in lattice units, but for the knot types 3_1^+, 6_2^+, 7_5^+, 8_2^+, 8_{15}^+, 9_2^+, 10_1^+ and 10_2^+ this exceeds 4 lattice units.

The minimal value of V_b is listed in the last column of table 3. This shows for example that a trefoil can be tied in the cubic lattice in a rectangular box of volume 16. Comparison of the results in this list shows that amongst 6 crossings knots it is 6_1^+ which can be tied in the smallest box, and amongst 7 crossings knots 7_1^+. In the list of 8 crossings prime knots, type 8_3 can be tied in a box of volume 27, far smaller than any other 8 crossing knot (or even any 5, 6 or 7 crossing knot). This suggests that 8_3 can be embedded very efficiently, using relatively little volume, in the SC lattice.

Knot	$\beta(0)$	p_m	$\max\beta(p)$	loc p_m	local $\max\beta(p)$	$\mathcal{W}_K$	Min V_b
0_1	0	–	–	–	–	0	0
3_1^+	0.65347	0.13557	0.92845	1.82115	0.05888	4.93207	16
4_1	0.43228	0.14599	0.64617	–	–	1.44036	27
5_1^+	0.82695	0	0.82695	1.43622	0.03260	3.32504	30
5_2^+	0.66116	0.13237	1.22294	–	–	3.28091	30
6_1^+	0.20546	0.22958	0.81816	–	–	2.65481	36
6_2^+	0.65497	0.09103	0.94525	1.20977	0.04840	5.14166	45
6_3	1.18846	0.04119	1.33719	–	–	2.10684	45
7_1^+	1.43410	0.06558	1.93627	–	–	1.55110	40
7_2^+	1.56522	0	1.56522	–	–	2.76117	45
7_3^+	0	–	–	–	–	0	45
7_4^+	0.05340	0	0.05340	–	–	0.33647	60
7_5^+	0.11667	0.23179	1.28010	–	–	5.28320	45
7_6^+	0.97333	0.03759	1.07580	–	–	2.18183	60
7_7^+	0.76190	0.05029	0.89165	–	–	1.09861	64
8_1^+	1.31169	0.04611	1.49428	–	–	3.56449	48
8_2^+	2.49340	0	2.49340	–	–	4.61042	48
8_3	3.98158	0	3.98158	–	–	2.12193	27
8_4^+	0.23441	0.18360	1.03728	–	–	3.68587	60
8_5^+	0	–	–	–	–	0	80
8_6^+	0	–	–	–	–	0	80
8_7^+	0	–	–	–	–	0	60
8_8^+	0	–	–	–	–	0	80
8_9	0.60841	0.09961	1.43594	–	–	1.99470	60
8_{10}^+	0	–	–	–	–	0	80
8_{11}^+	0	–	–	–	–	0	80
8_{12}	1.21212	0.04185	1.43594	–	–	1.09861	60
8_{13}^+	1.78904	0	1.78904	–	–	1.62612	64
8_{14}^+	0	–	–	–	–	0	80
8_{15}^+	2.36553	0	2.36553	–	–	4.45076	48
8_{16}^+	0	–	–	–	–	0	80
8_{17}	1.26959	0.04260	1.43108	–	–	3.54458	64
8_{18}	0	–	–	–	–	0	100
8_{19}^+	1.16978	0.04525	1.34959	–	–	2.09152	45
8_{20}^+	0	–	–	–	–	0	60
8_{21}^+	0.36279	0.15514	0.95539	–	–	2.33082	48
9_1^+	2.99129	0	2.99129	–	–	1.62095	50
9_2^+	1.97047	0	1.97047	0.40139	0.60045	7.39488	48
9_{42}^+	0.80392	0	0.80392	–	–	2.00459	60
9_{47}^+	1.81376	0	1.81376	–	–	0.26236	80
10_1^+	1.66066	0	1.66066	0.18995	0.98320	6.97624	54
10_2^+	3.12685	0	3.12685	–	–	4.57009	60

Table 3. Compressibility of SC Lattice Knots with volume V_b.

In table 4 the compressibilities of minimal SC lattices knots with the choice of the volume V_e are displayed. Generally, the compressibilities are smaller than those in table 3 – this is to be expected because the average excluded volume V_e is a more tightly fitting volume about the lattice knots, compared to the rectangular box volume V_b. All the minimal lattice knots in table 4 are compressible, with the exception of the unknot and the knot type 8_7^+. The largest compressibility is obtained for knot type 10_1^+ at $p = 1.29256\ldots$ where $\beta = 0.33799\ldots$. In knot types such as 10_1^+, the compressibility varies dramatically with pressure, and this example is illustrated in figure 12. A similar profile can be plotted for 9_{47}^+. The largest compressibility at zero pressure is found for knot type 10_2^+. Observe that there are no knot types with a

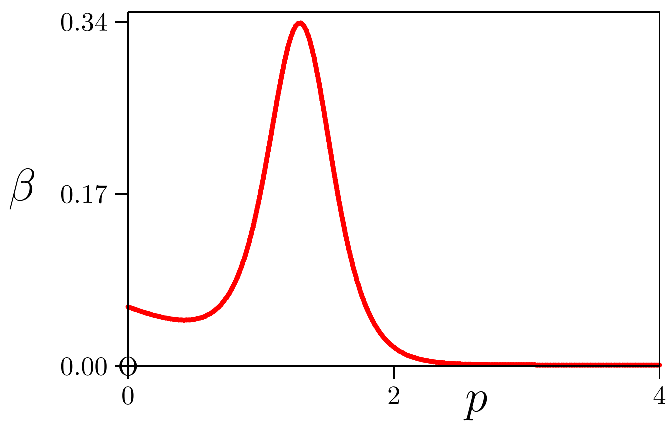

Figure 12. Compressibility of the SC minimal lattice knot of type 10_1^+ in its averaged excluded volume V_e.

secondary local maximum in the compressibility in table 4. Most knot types have maximum useful work between 0 and 6 in lattice units, but for the knot types 5_2^+, 6_2^+, 7_1^+, 7_2^+, 8_1^+, 8_2^+, 8_4^+, 8_9, 8_{13}^+, 8_{15}^+, 8_{19}^+, 8_{21}^+, 9_1^+, 9_2^+, 10_1^+ and 10_2^+ this exceeds 6 lattice units. The knot type 9_2^+ has particularly large value for the work, namely $\mathcal{W}_{9_2^+} = 11.13255\ldots$ far larger than types 10_1^+ and 10_2^+, where the work exceeds 9 units.

The minimal value of V_e is listed in the last column of table 4. The minimal value for 3_1^+ is 8, which is only one half of the volume of the minimal size rectangular box containing a lattice knot of type 3_1^+. This shows that the volume V_e is far smaller than V_b for this knot type, and the averaged excluded volume of the knot type is a far tighter fit about the lattice knot. Comparison of the results in this list shows similarly that 8_3 can be tied with relatively very small value of V_e, in this case $V_e = 12$, smaller than the minimal value of V_e for any other 5, 6, 7 or 8 crossing minimal lattice knots.

3.3. Compressibility of minimal lattice knots in the FCC and BCC lattices

The compressibility of minimal lattice knots in the FCC lattice can similarly be computed, using again two choices of an enclosing volume, namely V_b for the volume of the minimal rectangular box containing the polygon, and V_e for the volume of the average excluded volume.

The partition functions of FCC minimal lattice knots up to crossing number 7 and with volumes V_b are listed in table 5. With the choice of the average excluded volume

Knot	$\beta(0)$	p_m	$\max\beta(p)$	loc p_m	local $\max\beta(p)$	$\mathcal{W}_K$	Min V_e
0_1	0	–	–	–	–	0	0
3_1^+	0.05167	0.61046	0.05907	–	–	4.93207	8
4_1	0.02684	1.22731	0.03290	–	–	3.63759	12
5_1^+	0.01159	1.43811	0.01308	–	–	4.93447	14
5_2^+	0.04600	1.11177	0.06718	–	–	7.78072	44/3
6_1^+	0.02500	0.61768	0.02724	–	–	5.54518	37/2
6_2^+	0.03982	0.66098	0.04609	–	–	6.52796	113/6
6_3	0.05438	0.37398	0.05989	–	–	4.30407	37/2
7_1^+	0.03748	0.15097	0.03787	–	–	6.56174	121/6
7_2^+	0.05004	0.02186	0.05005	–	–	8.85474	85/4
7_3^+	0.00354	0.53600	0.00357	–	–	2.30259	65/3
7_4^+	0.00706	0.93823	0.00819	–	–	1.25276	68/3
7_5^+	0.01311	1.95942	0.04274	–	–	5.28320	68/3
7_6^+	0.03711	0	0.03711	–	–	5.87071	143/6
7_7^+	0.03062	0.56027	0.03859	–	–	1.65823	139/6
8_1^+	0.06928	0	0.06928	–	–	6.20355	73/3
8_2^+	0.07573	0	0.07573	–	–	7.55486	293/12
8_3	0.02684	1.22731	0.03290	–	–	3.63759	12
8_4^+	0.03488	0.53631	0.03840	–	–	6.21160	311/12
8_5^+	0.01102	0.08509	0.01103	–	–	3.17805	167/6
8_6^+	0.01169	0.63470	0.01226	–	–	5.43808	167/6
8_7^+	0	—	—	–	–	0	77/3
8_8^+	0.01758	0	0.01758	–	–	3.48124	57/2
8_9	0.04620	0.55186	0.05906	–	–	6.59987	79/3
8_{10}^+	0.00935	0.47816	0.00954	–	–	3.55535	28
8_{11}^+	0.00299	0.01757	0.00299	–	–	0.69315	169/6
8_{12}	0.01639	0.47743	0.01709	–	–	3.98898	83/3
8_{13}^+	0.05487	0.17977	0.05581	–	–	6.29895	161/6
8_{14}^+	0.00514	0.23152	0.00516	–	–	2.70805	169/6
8_{15}^+	0.05797	0.77810	0.07990	–	–	7.42118	76/3
8_{16}^+	0.00367	0.01653	0.00367	–	–	0.69315	359/12
8_{17}	0.03236	1.33662	0.03686	–	–	5.62402	343/12
8_{18}	0.01720	0.53164	0.01797	–	–	3.61092	377/12
8_{19}^+	0.06651	0.47415	0.08667	–	–	6.36819	107/6
8_{20}^+	0.00291	0.60279	0.00298	–	–	1.60944	275/12
8_{21}^+	0.05177	0.54428	0.05510	–	–	7.06262	263/12
9_1^+	0.07013	0.31127	0.07755	–	–	8.88288	103/4
9_2^+	0.04825	0.66653	0.05275	–	–	11.13255	169/6
9_{42}^+	0.02316	0.12142	0.02312	–	–	6.36130	289/12
9_{47}^+	0.02259	1.15783	0.19259	–	–	5.65599	101/4
10_1^+	0.05728	1.29256	0.33799	–	–	9.17347	83/3
10_2^+	0.07893	0	0.07893	–	–	9.11339	377/12

Table 4. Compressibility of SC Lattice Knots with volume V_e.

Knot	$Z_n(p)$
0_1	8
3_1^+	$16e^{-27p}+48e^{-24p}$
4_1	$24e^{-64p}+576e^{-48p}+348e^{-45p}+1416e^{-36p}+192e^{-32p}+48e^{-30p}+192e^{-27p}$
5_1^+	$48e^{-48p}+24e^{-45p}+24e^{-36p}$
5_2^+	$48e^{-80p}+96e^{-64p}+192e^{-60p}+288e^{-48p}+96e^{-45p}+48e^{-40p}$
6_1^+	$48e^{-125p}+816e^{-100p}+144e^{-96p}+4224e^{-80p}+1104e^{-75p}+912e^{-72p}$
	$+2448e^{-64p}+5712e^{-60p}+816e^{-54p}+2112e^{-48p}+624e^{-45p}+48e^{-40p}$
6_2^+	$960e^{-80p}+288e^{-75p}+48e^{-72p}+864e^{-64p}+1344e^{-60p}+1152e^{-48p}+384e^{-45p}$
6_3	$960e^{-100p}+48e^{-96p}+18336e^{-80p}+4896e^{-75p}+1440e^{-72p}+24096e^{-64p}+24864e^{-60p}$
	$+96e^{-54p}+23280e^{-48p}+3840e^{-45p}+864e^{-36p}$
7_1^+	$336e^{-100p}+2400e^{-80p}+144e^{-75p}+96e^{-72p}+192e^{-64p}+864e^{-60p}+48e^{-54p}$
7_2^+	$48e^{-120p}+432e^{-100p}+96e^{-96p}+96e^{-90p}+1200e^{-80p}+552e^{-75p}+432e^{-72p}+336e^{-64p}$
	$+672e^{-60p}+168e^{-54p}+96e^{-45p}$
7_3^+	$96e^{-100p}+96e^{-96p}+288e^{-80p}+96e^{-75p}+144e^{-72p}+48e^{-64p}+192e^{-60p}$
7_4^+	$72e^{-100p}+24e^{-96p}$
7_5^+	$144e^{-125p}+624e^{-120p}+6192e^{-100p}+1920e^{-96p}+720e^{-90p}+8112e^{-80p}+2544e^{-75p}$
	$+1488e^{-72p}+2064e^{-64p}+3216e^{-60p}+432e^{-54p}$
7_6^+	$480e^{-100p}+1728e^{-80p}+96e^{-75p}+1728e^{-64p}+288e^{-60p}+576e^{-48p}$
7_7^+	$96e^{-100p}+384e^{-80p}+48e^{-72p}+384e^{-64p}+192e^{-60p}+192e^{-48p}$

Table 5. Partition Functions: Minimal FCC lattice knots pressurized in a rectangular box.

the partition functions are similarly more complicated, and we do not reproduce those here.

The partition function of minimal lattice knots in the BCC lattice with the volume V_b is similarly given in table 6. Far more lengthy expressions are obtained when the average excluded volume V_e is used.

3.3.1. Compressibility of 3_1^+ in the FCC and BCC lattice: Considering first the cases with the rectangular box volume V_b, the partition functions of minimal length lattice trefoils in the FCC and BCC lattices evaluate to

$$\begin{aligned}\mathcal{Z}_{FCC}(3_1^+) &= 16e^{-27p}+48e^{-24p};\\ \mathcal{Z}_{BCC}(3_1^+) &= 24\,\mathrm{e}^{-125\,p}+480\,\mathrm{e}^{-100\,p}+696\,\mathrm{e}^{-80\,p}+384\,\mathrm{e}^{-75\,p}.\end{aligned}$$

The expected volume of the lattice minimal knot at pressure p is

$$\langle V_b\rangle = 3\left[\frac{\mathrm{e}^{-51\,p}}{(3\,\mathrm{e}^{-27\,p}+8\,\mathrm{e}^{-24\,p})\,(\mathrm{e}^{-27\,p}+3\,\mathrm{e}^{-24\,p})}\right]$$

in the FCC lattice, and

$$\langle V_b\rangle = 5\left[\frac{25\,\mathrm{e}^{-125\,p}+400\,\mathrm{e}^{-100\,p}+464\,\mathrm{e}^{-80\,p}+240\,\mathrm{e}^{-75\,p}}{\mathrm{e}^{-125\,p}+20\,\mathrm{e}^{-100\,p}+29\,\mathrm{e}^{-80\,p}+16\,\mathrm{e}^{-75\,p}}\right]$$

in the BCC lattice.

The compressibilities in these cases are given by

$$\beta = 3\left[\frac{\mathrm{e}^{-51\,p}}{(3\,\mathrm{e}^{-27\,p}+8\,\mathrm{e}^{-24\,p})\,(\mathrm{e}^{-27\,p}+3\,\mathrm{e}^{-24\,p})}\right]$$

Knot	$Z_n(p)$
0_1	$6\,e^{-8\,p} + 6\,e^{-4\,p}$
3_1^+	$24\,e^{-125\,p} + 480\,e^{-100\,p} + 696\,e^{-80\,p} + 384\,e^{-75\,p}$
4_1	$12\,e^{-80\,p}$
5_1^+	$48\,e^{-210\,p} + 624\,e^{-180\,p} + 792\,e^{-175\,p} + 432\,e^{-168\,p} + 4896\,e^{-150\,p} + 1776\,e^{-144\,p}$
	$+2736\,e^{-140\,p} + 264\,e^{-125\,p} + 1536\,e^{-120\,p} + 504\,e^{-112\,p} + 456\,e^{-108\,p} + 768\,e^{-105\,p}$
5_2^+	$144\,e^{-180\,p} + 144\,e^{-175\,p} + 2064\,e^{-150\,p} + 48\,e^{-144\,p} + 912\,e^{-140\,p} + 24\,e^{-125\,p} + 1056\,e^{-120\,p}$
	$+480\,e^{-112\,p}$
6_1^+	$48\,e^{-150\,p} + 24\,e^{-112\,p}$
6_2^+	$336\,e^{-216\,p} + 3600\,e^{-180\,p} + 576\,e^{-175\,p} + 3168\,e^{-150\,p} + 432\,e^{-144\,p} + 144\,e^{-125\,p}$
6_3	$48\,e^{-210\,p} + 528\,e^{-180\,p} + 240\,e^{-168\,p} + 1968\,e^{-150\,p} + 336\,e^{-144\,p} + 144\,e^{-125\,p} + 48\,e^{-120\,p}$
7_1^+	$24\,e^{-252\,p} + 144\,e^{-216\,p} + 144\,e^{-210\,p} + 936\,e^{-180\,p} + 216\,e^{-175\,p}$
7_2^+	$24\,e^{-180\,p}$
7_3^+	$48\,e^{-294\,p} + 480\,e^{-252\,p} + 144\,e^{-245\,p} + 1632\,e^{-240\,p} + 144\,e^{-225\,p} + 720\,e^{-216\,p}$
	$+9312\,e^{-210\,p} + 4128\,e^{-200\,p} + 3000\,e^{-180\,p} + 1152\,e^{-175\,p} + 384\,e^{-168\,p} + 816\,e^{-160\,p}$
	$+48\,e^{-150\,p} + 480\,e^{-144\,p}$
7_4^+	$24\,e^{-343\,p} + 480\,e^{-294\,p} + 2016\,e^{-252\,p} + 1008\,e^{-245\,p} + 912\,e^{-216\,p} + 2592\,e^{-210\,p}$
	$+144\,e^{-196\,p} + 48\,e^{-192\,p} + 2544\,e^{-180\,p} + 1008\,e^{-175\,p} + 48\,e^{-168\,p} + 384\,e^{-150\,p}$
7_5^+	$48\,e^{-252\,p} + 192\,e^{-240\,p} + 144\,e^{-225\,p} + 144\,e^{-216\,p} + 1872\,e^{-210\,p} + 1632\,e^{-200\,p}$
	$+2688\,e^{-180\,p} + 528\,e^{-175\,p} + 192\,e^{-168\,p} + 816\,e^{-160\,p} + 48\,e^{-150\,p} + 480\,e^{-144\,p}$
7_6^+	$48\,e^{-150\,p}$
7_7^+	$24\,e^{-144\,p}$

Table 6. Partition Functions: Minimal BCC lattice knots pressurized in a rectangular box.

in the FCC lattice, and

$$\beta = 5\left[\frac{500\,e^{-225\,p} + 2349\,e^{-205\,p} + 1600\,e^{-200\,p} + 9280\,e^{-180\,p} + 8000\,e^{-175\,p} + 464\,e^{-155\,p}}{\left(25\,e^{-125\,p} + 400\,e^{-100\,p} + 464\,e^{-80\,p} + 240\,e^{-75\,p}\right) A}\right]$$

in the BCC lattice, where $A = \left(e^{-125\,p} + 20\,e^{-100\,p} + 29\,e^{-80\,p} + 16\,e^{-75\,p}\right)$.

Plotting these compressibilities in the FCC and BCC lattices for $p \in [0,2]$ gives the curves in figure 13. If the average excluded volume V_e is used instead, then the partition functions of minimal length lattice trefoils in the FCC and BCC lattices are

$$\mathcal{Z}_{FCC}(3_1^+) = 64\,e^{-13/2\,p}; \tag{4}$$

$$\begin{aligned}\mathcal{Z}_{BCC}(3_1^+) = {} & 168\,e^{-16\,p} + 240\,e^{-\frac{52}{3}\,p} + 432\,e^{-\frac{50}{3}\,p} + 144\,e^{-\frac{53}{3}\,p} \\ & + 288\,e^{-17\,p} + 72\,e^{-18\,p} + 96\,e^{-\frac{55}{3}\,p} + 24\,e^{-\frac{56}{3}\,p} \\ & + 96\,e^{-\frac{47}{3}\,p} + 24\,e^{-\frac{44}{3}\,p}.\end{aligned} \tag{5}$$

The expected volume of the minimal lattice trefoil at pressure p is equal to $\langle V_e \rangle = 13/2$ (independent on p) in the FCC lattice, and is a lengthy expression (dependent on p) in the BCC lattice. The compressibility in the FCC lattice is identically zero, and in the BCC lattice is again a lengthy expression. Plotting these compressibilities in the FCC and BCC lattices for $p \in [0,2]$ gives the curves in figure 13(b).

Observe that for both choices of the volumes V_b and V_e, that 3_1^+ is more compressible in the BCC lattice than in the FCC lattice. This observation shows

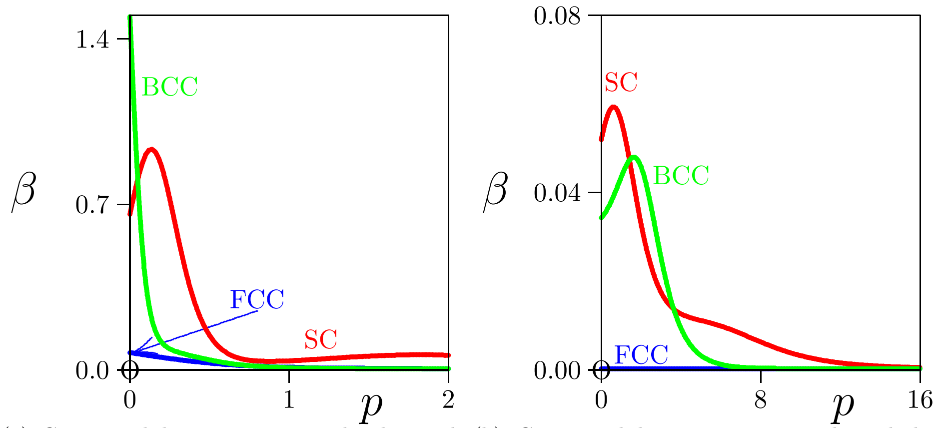

(a) Compressibility in a rectangular box volume V_b. (b) Compressibility in a averaged excluded volume V_e.

Figure 13. Compressibility of the minimal lattice knots of type 3_1^+ in the FCC and BCC lattices. The compressibility in the SC lattice (see figures 2 and 8) are included for comparison.

that the knot is much more tightly embedded in the FCC lattice, and that increasing pressure compress the knot less in the FCC lattice.

The global maxima of β in figure 13(a) (this is for the choice V_b) occurs at $p = 0$ in the FCC and BCC lattices. In this particular case, $\beta = 1.17690\ldots$ in the FCC lattice and $\beta = 1.48918\ldots$ in the BCC lattice at zero pressure. The compressibility decreases monotonically with increasing $p > 0$ in both cases. If the volume V_e is used instead, then $\beta = 0$ for $p \geq 0$ in the FCC lattice (the lattice knot is incompressible), but there is a global maximum in β at $p = 1.62452\ldots$ where $\beta = 0.04773\ldots$.

The maximum amount of useful work that can be performed by letting a lattice knot type 3_1^+ expand from its maximal compressed state to its equilibrium at zero pressure in the FCC and BCC lattices can be computed as before. In these lattices, $\mathcal{W}_{3_1^+} = \log(4/3) = 0.28768\ldots$ in the FCC lattice, and $\mathcal{W}_{3_1^+} = \log(33/8) = 1.41707\ldots$ in the BCC lattice. If V_e is used instead, then $\mathcal{W}_{3_1^+} = 0$ in the FCC lattice, and $\mathcal{W}_{3_1^+} = \log 66 = 4.18965\ldots$ in the BCC lattice.

3.3.2. The compressibility of minimal lattice knots in the FCC and BCC lattices: The compressibilities of the figure eight knot 4_1 are illustrated in the FCC and BCC lattices for the choices of the volumes V_b and V_e in figures 14. For the choice of volume V_b in the FCC lattice, the maximum compressibility of 4_1 is at $p = 0$, when $\beta = 1.17690\ldots$, but for V_e one obtains a maximum at $p = 0.86318\ldots$ where $\beta = 0.07938\ldots$. The knot is incompressible for both choices V_b and V_e in the BCC lattice.

The maximum amount of work is $\mathcal{W}_{4_1} = \log(233/16) = 2.67844\ldots$ in the FCC lattice for V_b, and $\mathcal{W}_{4_1} = \log(233/8) = 3.37159\ldots$ in the FCC lattice with the choice V_e.

Data on the compressibility of lattice knots in the FCC lattice with the choice of volume V_b is given in table 7 and with the choice of volume V_e in table 8. Observe that in most cases the maximal compressibility is at zero pressure, and that exceptions to this are sporadic in tables 7 and 8. Even more sporadic are knot types with secondary

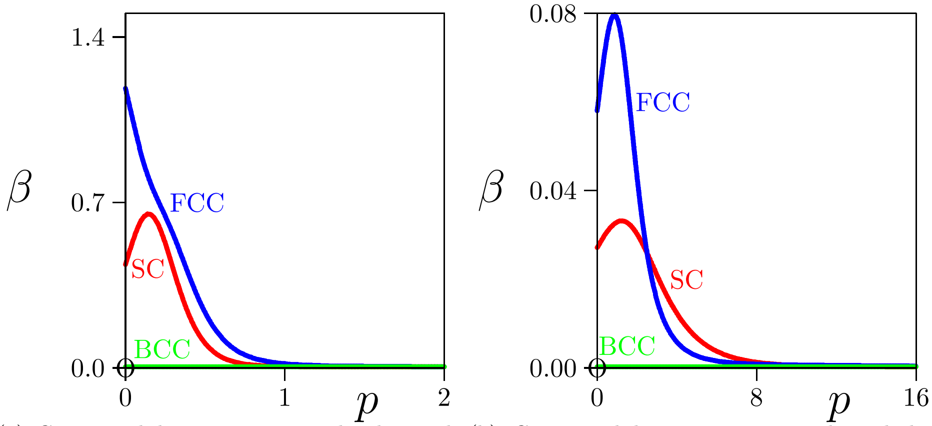

(a) Compressibility in a rectangular box volume V_b.

(b) Compressibility in a averaged excluded volume V_e.

Figure 14. Compressibility of the minimal lattice knots of type 4_1 in the FCC and BCC lattices. The compressibilities in the SC lattice (see figure 9) are included for comparison.

local maxima in the compressibility, as seen for example in figure 2 for the trefoil knot – in fact, with the choice of volume V_b only the knot types 7_1^+ and 8_{11}^+ have secondary local maximum in the compressibility, and with V_e, only 8_{18}.

Amongst knot types of 8 crossing the knot types 8_{18}, 8_{19}^+ and 8_{20}^+ can be realised in a rectangular box of volume 45, small compared with the other eight crossing knots. This is only slightly smaller than the minimum value of V_b for 8_1^+, which is 48.

The maximum work in table 7 is obtained for 8_1^+, and $\mathcal{W}_{8_1^+} = 8.44779\ldots$. Other knot types which have high values for $\mathcal{W}_K$ are 6_1^+, 8_2^+, 8_{11}^+, 8_{13}^+, 8_{20}^+ and 9_2^+.

If one considers the volume V_e instead, then there is a steady increase of V_e with increasing knot complexity in table 8. The maximum work in table 8 is obtained for 8_1^+, and $\mathcal{W}_{8_1^+} = 9.14094\ldots$. Other knot types which have high values for $\mathcal{W}_K$ are 6_3, 8_2^+, 8_{11}^+, 8_{13}^+, 9_2^+ and 10_1^+.

Data on the compressibility of lattice knots in the BCC lattice with the choice of volume V_b are given in table 9 and with the choice of volume V_e in table 10.

In most cases the maximal compressibility is at zero pressure, but there are some exceptions to this in tables 9 and 10. For example, the maximum compressibility of the unknot is at $p = 0.08664\ldots$ for the choice V_b in table 9.

There are also some knot types with secondary local maxima in the compressibility, similar to the case seen in figure 2 for the trefoil in the SC lattice with the choice of V_b as volume. With the choice V_b in the BCC, these include 6_3, 7_1^+, 8_4^+, 8_7^+, 8_9, 8_{18}, 9_2^+ and 9_{47}^+, and for the choice V_e, 6_2^+, 7_3^+ and 9_2^+.

Amongst knot types of eight crossings the knot types 8_1^+, 8_3, 8_{12}, 8_{18} and 8_{19}^+ can be realised in a rectangular box of volume 144; this is smaller than other eight crossing knots, and these knot types have compact minimal length conformations in the BCC. As one would expect, with some exceptions, these knot types are also less compressible than eight crossing knots.

The maximum work in table 9 is obtained for 8_4^+, and $\mathcal{W}_{8_4^+} = 7.57968\ldots$. Other knot types which have high values for $\mathcal{W}_K$ are 8_2^+, 8_7^+ and 8_{18}.

Knot	$\beta(0)$	p_m	$\max\beta(p)$	loc p_m	loc $\max\beta(p)$	$\mathcal{W}_K$	Min V_b
0_1	0	–	–	–	–	0	0
3_1^+	0.06818	0	0.06818	–	–	0.28768	24
4_1	1.17690	0	1.17690	–	–	2.67845	27
5_1^+	0.54661	0.10381	0.72940	–	–	1.38629	36
5_2^+	1.84036	0	1.84036	–	–	2.77259	40
6_1^+	2.78110	0	2.78110	–	–	5.98141	40
6_2^+	2.28512	0	2.28512	–	–	2.57452	45
6_3	2.31350	0	2.31350	–	–	4.77819	36
7_1^+	1.63106	0.02343	1.65022	0.46211	0.17066	4.44265	54
7_2^+	2.63144	0	2.63144	–	–	3.76120	45
7_3^+	2.10233	0	2.10233	–	–	1.60944	60
7_4^+	0.03030	0.27976	0.04082	–	–	1.38629	96
7_5^+	2.86502	0	2.86502	–	–	4.15191	54
7_6^+	2.77693	0	2.77693	–	–	2.14007	48
7_7^+	2.79374	0	2.79374	–	–	1.90954	48
8_1^+	3.54811	0	3.54811	–	–	8.44779	48
8_2^+	3.08699	0	3.08699	–	–	5.59306	54
8_3	3.39870	0	3.39870	–	–	3.10109	60
8_4^+	3.35418	0	3.35418	–	–	3.75654	60
8_5^+	1.21929	0	1.21929	–	–	3.43399	63
8_6^+	3.92441	0	3.92441	–	–	3.08089	60
8_7^+	1.61860	0	1.61860	–	–	1.46634	64
8_8^+	2.82549	0	2.82549	–	–	2.06369	60
8_9	3.13220	0	3.13220	–	–	2.60269	60
8_{10}^+	2.03727	0	2.03727	–	–	0.81093	80
8_{11}^+	3.10730	0	3.10730	0.58372	0.18936	8.04093	54
8_{12}	3.14959	0.00838	3.16225	–	–	2.65676	60
8_{13}^+	3.25299	0	3.25299	–	–	5.24965	48
8_{14}^+	3.07391	0	3.07391	–	–	2.12613	60
8_{15}^+	2.67195	0	2.67195	–	–	4.84024	60
8_{16}^+	1.88507	0	1.88507	–	–	1.21640	64
8_{17}	1.81676	0	1.81676	–	–	1.21640	64
8_{18}	3.11696	0.01503	3.16790	–	–	3.28916	45
8_{19}^+	0.25869	0.17760	1.50198	–	–	3.13549	45
8_{20}^+	1.73255	0	1.73255	–	–	5.95551	45
8_{21}^+	2.06897	0	2.06897	–	–	2.39253	60
9_1^+	2.00000	0.01014	2.02041	–	–	1.38629	80
9_2^+	3.82335	0	3.82335	–	–	5.21577	60
9_{42}^+	0	–	–	–	–	0	80
9_{47}^+	0.92683	0.10758	1.04061	–	–	2.36712	64
10_1^+	4.11636	0	4.11636	–	–	4.13116	80
10_2^+	4.42190	0	4.42190	–	–	3.02852	80

Table 7. Compressibility of FCC Lattice Knots with volume V_b.

Knot	$\beta(0)$	p_m	$\max \beta(p)$	loc p_m	loc $\max \beta(p)$	$\mathcal{W}_K$	Min V_e
0_1	0	–	–	–	–	0	0
3_1^+	0	–	–	–	–	0	13/2
4_1	0.05773	0.86318	0.07939	–	–	3.37160	61/6
5_1^+	0.01793	1.00305	0.02393	–	–	1.38629	37/3
5_2^+	0.02808	0.39566	0.02899	–	–	2.77259	85/6
6_1^+	0.05461	0.18826	0.05525	–	–	5.98141	101/6
6_2^+	0.06128	0.57204	0.07799	–	–	4.65396	33/2
6_3	0.03845	1.33926	0.07523	–	–	6.97541	107/6
7_1^+	0.03763	1.23906	0.05985	–	–	4.44265	56/3
7_2^+	0.04219	0.81100	0.05525	–	–	4.45435	41/2
7_3^+	0.02067	0	0.02067	–	–	2.99573	22
7_4^+	0	–	–	–	–	0	59/3
7_5^+	0.04597	0.83134	0.06570	–	–	6.34914	127/6
7_6^+	0.02878	0.60837	0.03174	–	–	4.62497	23
7_7^+	0.00706	0	0.00706	–	–	2.60269	149/6
8_1^+	0.07131	0.83333	0.08379	–	–	9.14094	68/3
8_2^+	0.07810	0.70937	0.11184	–	–	7.09714	70/3
8_3	0.05429	0.24897	0.05568	–	–	5.99146	51/2
8_4^+	0.07784	0.64740	0.13305	–	–	6.05912	23
8_5^+	0.03590	0.05611	0.03594	–	–	4.82028	27
8_6^+	0.05098	0	0.05098	–	–	5.27811	157/6
8_7^+	0.01714	1.00129	0.02788	–	–	3.25810	80/3
8_8^+	0.02133	0	0.02133	–	–	4.14313	82/3
8_9	0.03862	0.99643	0.05810	–	–	4.68213	76/3
8_{10}^+	0.01719	0	0.01719	–	–	3.58352	55/2
8_{11}^+	0.04565	0.90466	0.05686	–	–	8.73408	76/3
8_{12}	0.04210	0.50800	0.04937	–	–	5.14166	82/3
8_{13}^+	0.05485	0.93825	0.08329	–	–	8.65085	149/6
8_{14}^+	0.02199	1.48654	0.02628	–	–	6.34564	167/6
8_{15}^+	0.03477	0.53993	0.03777	–	–	6.63200	163/6
8_{16}^+	0.02406	0.34559	0.02490	–	–	5.78074	85/3
8_{17}	0.01195	0.63042	0.01246	–	–	4.68213	29
8_{18}	0.04895	0	0.04895	0.85036	0.04679	6.06175	85/3
8_{19}^+	0.01621	1.02391	0.01949	–	–	3.13549	56/3
8_{20}^+	0.05023	0.98438	0.08007	–	–	6.24320	59/3
8_{21}^+	0.02566	1.25537	0.03751	–	–	5.91889	133/6
9_1^+	0.00758	0.03410	0.00758	–	–	1.38629	86/3
9_2^+	0.07279	0.67316	0.08113	–	–	8.47387	161/6
9_{42}^+	0.00028	0.02007	0.00028	–	–	0.69315	149/6
9_{47}^+	0.01177	0.45773	0.01190	–	–	4.15888	89/3
10_1^+	0.06685	0.55416	0.07921	–	–	7.38926	31
10_2^+	0.06372	0.45145	0.08370	–	–	5.22575	32

Table 8. Compressibility of FCC Lattice Knots with volumes V_e.

Knot	$\beta(0)$	p_m	$\max \beta(p)$	loc p_m	loc $\max \beta(p)$	$\mathcal{W}_K$	Min V_b
0_1	0.66667	0.08664	0.68629	–	–	0.69315	4
3_1^+	1.48918	0	1.48918	–	–	1.41707	75
4_1	0	–	–	–	–	–	80
5_1^+	2.58695	0.02790	2.78116	–	–	2.96075	105
5_2^+	2.08587	0.00813	2.09679	–	–	2.31747	112
6_1^+	2.33657	0.02208	2.77037	–	–	1.09861	112
6_2^+	2.06977	0	2.06977	–	–	4.04888	125
6_3	1.54825	0	1.54825	0.09268	1.34564	4.23411	120
7_1^+	1.37260	0	1.37260	0.28854	0.03530	1.91365	175
7_2^+	0	–	–	–	–	–	180
7_3^+	2.41600	0.04325	3.10143	–	–	3.84695	144
7_4^+	5.70413	0	5.70413	–	–	3.37374	150
7_5^+	2.49925	0.01719	2.56136	–	–	2.90690	144
7_6^+	0	–	–	–	–	–	150
7_7^+	0	–	–	–	–	–	144
8_1^+	2.25572	0.05046	5.70492	–	–	3.43399	144
8_2^+	3.20299	0	3.20299	–	–	7.11477	168
8_3	1.96612	0.03662	5.29029	–	–	2.19722	144
8_4^+	5.43599	0	5.43599	0.38809	0.10046	7.57968	168
8_5^+	3.14193	0	3.14193	–	–	2.01653	175
8_6^+	3.44004	0	3.44004	–	–	5.23644	160
8_7^+	3.37683	0	3.37683	0.10270	1.94863	6.90475	160
8_8^+	3.49969	0	3.49969	–	–	4.79027	168
8_9	2.59394	0	2.59394	0.05510	1.94102	3.16969	175
8_{10}^+	2.24347	0	2.24347	–	–	2.55205	180
8_{11}^+	2.41677	0	2.41677	–	–	5.80212	175
8_{12}	0	–	–	–	–	–	144
8_{13}^+	4.10106	0	4.10106	–	–	5.21221	168
8_{14}^+	3.13157	0	3.13157	–	–	5.86647	160
8_{15}^+	1.73039	0.05233	2.12601	–	–	3.39002	168
8_{16}^+	0.97928	0	0.97928	–	–	1.29928	175
8_{17}	0.92879	0	0.92879	–	–	0.30538	180
8_{18}	4.70675	0	4.70675	0.16392	2.02337	6.59987	144
8_{19}^+	1.69240	0.03863	2.08744	–	–	1.72385	144
8_{20}^+	3.41192	0	3.41192	–	–	4.96634	150
8_{21}^+	2.03630	0	2.03630	–	–	2.26868	175
9_1^+	4.05666	0	4.05666	–	–	5.92604	180
9_2^+	4.80856	0	4.80856	0.08777	2.46128	5.66296	168
9_{42}^+	1.80198	0	1.80198	–	–	3.34990	175
9_{47}^+	2.10389	0	2.10389	0.09644	1.64930	5.06189	175
10_1^+	3.33858	0	3.33858	–	–	1.79176	210
10_2^+	2.72186	0.01441	2.79899	–	–	2.14251	240

Table 9. Compressibility of BCC Lattice Knots with volumes V_b.

Knot	$\beta(0)$	p_m	$\max\beta(p)$	loc p_m	loc $\max\beta(p)$	$\mathcal{W}_K$	Min V_e
0_1	0	–	–	–	–	0	0
3_1^+	0.03402	1.62452	0.04773	–	–	4.18965	44/3
4_1	0	–	–	–	–	0	64/3
5_1^+	0.06553	1.22854	0.10245	–	–	5.32788	80/3
5_2^+	0.05674	0	0.05674	–	–	4.62006	91/3
6_1^+	0.00629	0	0.00629	–	–	0.40547	35
6_2^+	0.05241	0	0.05241	1.37261	0.03755	5.14749	116/3
6_3	0.03892	0.79096	0.05619	–	–	4.23411	116/3
7_1^+	0.03748	0	0.03748	–	–	1.71298	124/3
7_2^+	0	–	–	–	–	0	44
7_3^+	0.06347	0	0.06347	0.22071	0.06115	6.14954	134/3
7_4^+	0.09845	0.57690	0.38184	–	–	5.45318	40
7_5^+	0.06912	0	0.06912	–	–	5.20949	48
7_6^+	0	–	–	–	–	0	47
7_7^+	0	–	–	–	–	0	48
8_1^+	0.09074	0.23262	0.11279	–	–	2.74084	49
8_2^+	0.09247	0.71950	0.17808	–	–	7.80792	152/3
8_3	0.00856	0	0.00856	–	–	0.58779	152/3
8_4^+	0.13367	0.39542	0.26081	–	–	6.88653	148/3
8_5^+	0.07155	0	0.07155	–	–	5.03695	167/3
8_6^+	0.06902	0.65504	0.10783	–	–	5.23644	54
8_7^+	0.08047	0.57910	0.13155	–	–	6.90475	52
8_8^+	0.11540	0.46546	0.11558	–	–	6.58203	54
8_9	0.06412	0	0.06412	–	–	4.77912	169/3
8_{10}^+	0.04289	0.77248	0.05574	–	–	5.44242	166/3
8_{11}^+	0.07035	0.93770	0.07418	–	–	5.80212	166/3
8_{12}	0	–	–	–	–	0	176/3
8_{13}^+	0.05706	0.71565	0.07935	–	–	5.90536	56
8_{14}^+	0.09919	0	0.09919	–	–	5.86647	170/3
8_{15}^+	0.05556	0.86305	0.06846	–	–	4.48864	57
8_{16}^+	0.08002	0.19909	0.08208	–	–	3.09104	58
8_{17}	0.04271	0	0.04271	–	–	2.94444	58
8_{18}	0.16917	0	0.16917	–	–	5.21358	191/3
8_{19}^+	0.17811	0	0.17811	–	–	2.44777	42
8_{20}^+	0.11282	0.07141	0.11314	–	–	7.79955	134/3
8_{21}^+	0.04977	0	0.04977	–	–	2.67415	148/3
9_1^+	0.07219	0	0.07219	–	–	7.43011	57
9_2^+	0.08763	0	0.08763	0.89024	0.08575	5.66296	170/3
9_{42}^+	0.04013	0.46670	0.05049	–	–	4.04305	157/3
9_{47}^+	0.09375	0	0.09375	–	–	6.56597	63
10_1^+	0.05363	0.23863	0.06286	–	–	1.79176	64
10_2^+	0.06635	0.89586	0.09463	–	–	6.01372	200/3

Table 10. Compressibility of BCC Lattice Knots with volumes V_e.

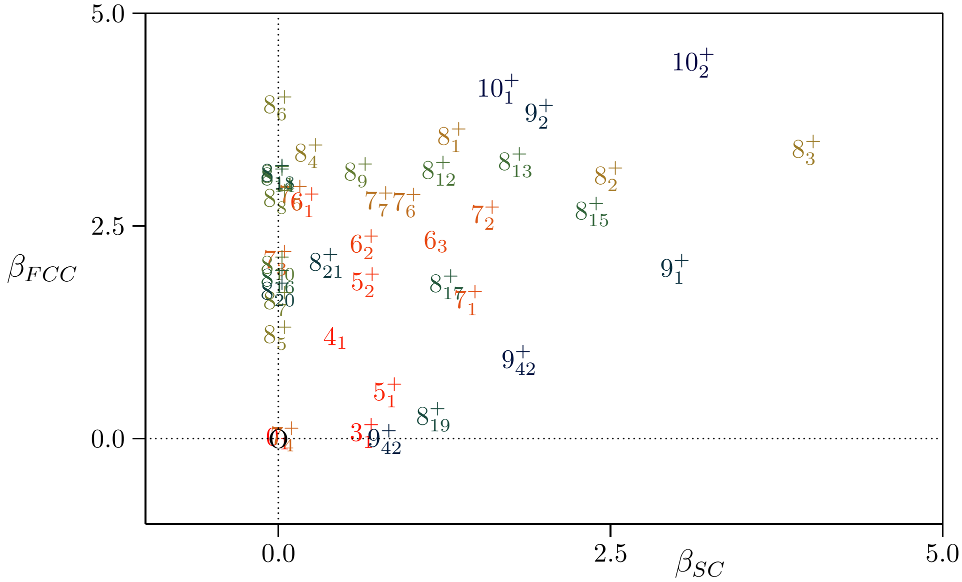

Figure 15. Scatter plot of zero pressure compressibilities (V_b) of minimal lattice knots in the SC and FCC lattices. Generally, the lattice knots are more compressible in the FCC, although there are exceptions to this, these would be the knot types which lay below the diagonal in this diagram.

If one considers the volume V_e instead, then there is a steady increase of V_e with increasing knot complexity in table 10. Amongst knot types of eight crossing the knot types 8_{19}^+ and 8_{20}^+ can be realised with averaged excluded volume V_e equal to 42 and 134/3, this is small when compared to other eight crossing knots.

The maximum work in table 10 is obtained for 8_2^+, and $\mathcal{W}_{8_2^+} = 7.80792\ldots$. Other knot types which has high values for $\mathcal{W}_K$ are 8_{20}^+ and 9_1^+.

3.4. Discussion of Results

The compressibility data of SC lattice knots in tables 3 and 4 indicate that different knot types may have very different properties. That is, the compressibilities are functions of the topologies of the embedded polygons, as well as of the geometry of the polygons, since the results are also dependent on the lattice, as seen for example when comparing the data in tables 3, 7 and 9.

Generally, the minimal length lattice knots were also more compressible in the volume V_b, compared to the average excluded volume V_e which is a more close-fitting envelope about the polygon. This should be due to the fact that there is extra space for the compressed polygon to expand into near the corners of the rectangular box in the volume V_b, and this is not available in the volume V_e.

There appears to the little correlation between the zero pressure compressibility of minimal lattice knots in the three lattices. For example, in figures 15 and 16 two scatter plots of the zero pressure compressibility computed from the rectangular box volume V_b are given, showing a wide dispersion of points and little correlation between the data in different lattices. There are some generic trends visible in these plots, for example, compressibility tends to increase with crossing number in at least one of

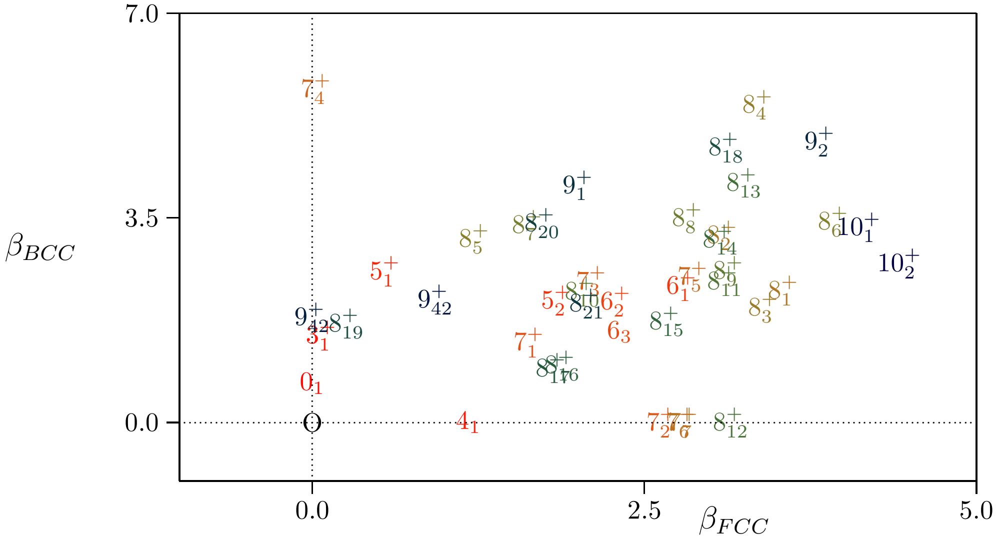

Figure 16. Scatter plot of zero pressure compressibilities (V_b) of minimal lattice knots in the FCC and BCC lattices. Generally, the lattice knots are more compressible in the FCC.

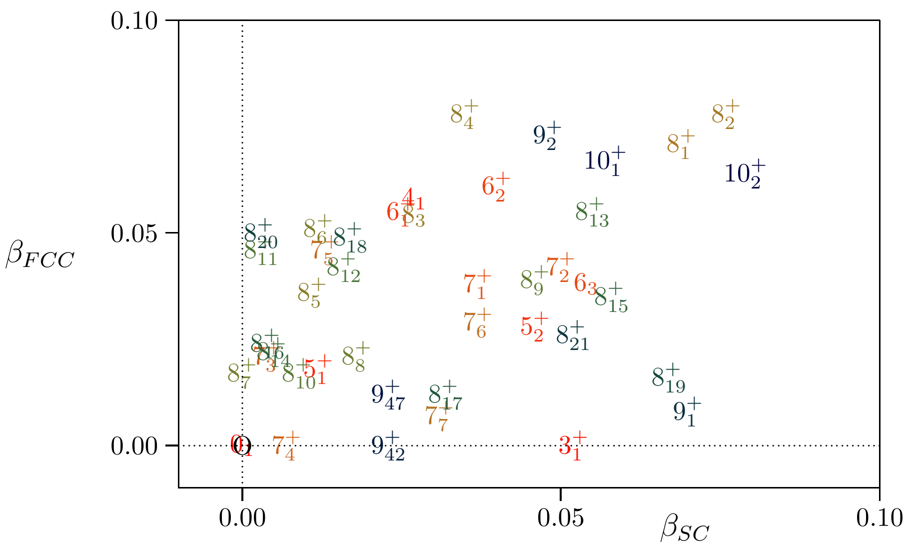

Figure 17. Scatter plot of zero pressure compressibilities of minimal lattice knots computed from the volume V_e in the FCC and BCC lattices.

the lattices (and knots with low crossing number are likely to be closer to the origin in these plots).

The situation is similar if the compressibilities are instead computed by consider the more close fitting volume V_e. In figure 17 a scatter plot of the zero pressure compressibilities in the SC and FCC lattices, computed from V_e, are illustrated. The wide dispersion of the points are similar to the results seen for the volume V_b.

Examination of the data on $\mathcal{W}_K$ in each of the lattices and for the knot types,

shows that there are some correlations between compressibility and the total amount of work. For example, in figure 18 a strong correlation is observed between the maximum compressibility β_m and $\mathcal{W}_K$ of knot types in the SC lattice computed from the volume V_e. Similar graphs are obtained in the other lattices and also for the choice of V_b as

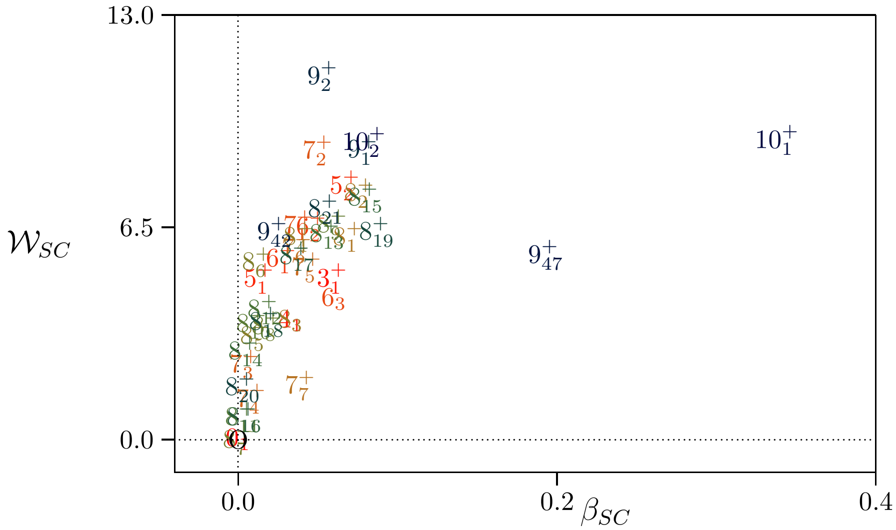

Figure 18. Scatter plot of maximum compressibilities of minimal lattice knots and the total amount of work $\mathcal{W}_L$ computed from the volume V_e in the SC lattice. The data show a close correlation, with the knot types 9_{47}^+ and 10_1^+ clear outliers in this graph.

containing volume. There are somewhat weaker correlations between zero pressure compressibility and $\mathcal{W}_K$ in all cases.

The data in tables 3, 7, 8, 9 and 10 show an association between knot types having secondary local maxima in their compressibility curves, and having high total value of $\mathcal{W}_K$. In table 3 the knot types 3_1^+, 5_1^+, 6_2^+, 9_2^+ and 10_1^+ have local maxima in β_{SC} (the case for 3_1^+ is illustrated in figure 2), and all have higher values of $\mathcal{W}_K$ than comparable knots. A similar pattern can be seen in the other other tables.

4. Conclusions

In this paper the compressibility of minimal length lattice knots were examined in three lattices, namely the SC, the FCC and the BCC lattices. Generally, the compressibility properties were found to be dependent on the lattice as well as the knot type. Since the lattice impose a geometric constraint on the lattice knots, the compressibility is determined to be a function of the geometry.

More generally, different knot types were also found to have very different compressibility properties in each of the lattices. This is for example illustrated in figure 10 and 11 for SC lattice knots; the compressibilities of knot types of roughly the same geometric and topological complexity (for example, about the same minimal length and with the same crossover numbers) are seen to have different compressibilities with increasing forces.

We examined the compressibilities by using two notions of a confining space for the lattice knots, firstly the smallest rectangular box volume V_b containing the polygons,

and secondly an average excluded volume V_e computed by slicing the knot in slabs, taking the convex hulls of those slabs, and then their union. V_e is a very tight envelope around the lattice knot.

In figure 6 we show that there is a strong correlation in knot type between V_b and V_e in the SC lattice, and the convex hull volume is thus similarly highly correlated with both V_b and V_e. Similar results were obtained in the FCC and BCC lattices. Thus, for many knot types the compressibilities β were similarly behaved for either choice of the volume, as one may see in figures 2 and 8 for the knot type 3_1 and in figure 9 for the knot type 4_1 in the SC lattice. This was not universally the case however, as for example seen in figure 13, where data in the three lattices are compared for the trefoil knot.

We do however see the following qualitative features in our results: (1) Compressibilities are not monotonic with increasing pressure, but may rise and fall instead, and may even exhibit two local maxima. That is, with increasing pressure the lattice knot may become relatively more compressible in the sense that fractional change in volume may increase with pressure in certain pressure ranges. (2) Generally, in tables 3 and 4, 7 and 8, and 9 and 10, there is a weak pattern of increasing compressibility at zero pressure down the tables. (3) We found that FCC lattice knots are likely to have larger compressibility with the volume V_b, as seen in figures 15 and 16, although there are many exceptions to this. This is not the case if the volume V_e is used, as one may for example see in figure 17.

We have also computed several other properties of the lattices knots, such as for example the minimum values of V_b and V_e in each case. In addition, the maximum amount of useful work that can be extracted from a knot if it undergoes a reversible isothermic expansion. This sets an upper bound on the amount of useful work that van be extracted by the expansion of a compressed lattice knot. Our results were listed and discussed (see for example figure 18).

Knot	$\beta(0)$	p_m	$\max\beta(p)$	loc p_m	loc $\max\beta(p)$	$\mathcal{W}_K$	Min V
$3_1^+\#3_1^+$	1.27231	0.33117	2.24876	–	–	7.15149	24
$3_1^+\#3_1^-$	1.51949	0.20408	1.25617	–	–	8.42508	24
$3_1^+\#4_1$	1.76227	0.00000	1.76227	–	–	4.79472	36
$4_1\#4_1$	2.30417	0.03292	2.57205	–	–	6.77072	45
$3_1^+\#5_1^+$	0.46721	0.19779	2.91011	–	–	6.03715	40
$3_1^+\#5_1^-$	1.50415	0.10167	1.73399	–	–	7.07741	40
$3_1^+\#5_2^+$	2.22590	0.00000	2.22590	–	–	9.99405	40
$3_1^+\#5_2^-$	0.12513	0.24702	0.66874	–	–	2.90872	48
$3_1^+\#3_1^+$	0.04653	0.89401	0.71536	–	–	6.45834	53/4
$3_1^+\#3_1^-$	0.05839	1.28041	0.13051	–	–	8.42508	97/6
$3_1^+\#4_1$	0.05482	0.96456	0.07746	–	–	8.22871	259/12
$4_1\#4_1$	0.06322	1.42818	0.09618	–	–	8.85016	51/2
$3_1^+\#5_1^+$	0.04639	1.28800	0.11847	–	–	8.33974	70/3
$3_1^+\#5_1^-$	0.04577	1.40675	0.10193	–	–	9.38000	91/4
$3_1^+\#5_2^+$	0.07706	1.31128	0.16266	–	–	11.24682	70/3
$3_1^+\#5_2^-$	0.03321	0.95426	0.05034	–	–	4.00733	101/4

Table 11. Compressibility of Compound SC Lattice Knots with volumes V_b (top data) and V_e (bottom data).

As a final set of calculations, we considered minimal length lattice knots with compound knot type in the SC lattices. Our results are listed in table 11. Note that in this short list for both choices of the volume (V_b or V_e) that $3_1^+\#5_2^+$ is the most compressible and has the largest value for $\mathcal{W}_K$. Similarly, $3_1^+\#5_2^-$ is the least compressible with the lowest value of $\mathcal{W}_K$.

Acknowledgements: The authors acknowledge support in the form of NSERC grants from the Government of Canada.

Bibliography

[1] Aragão de Carvalho C and Caracciolo S 1983 *A New Monte Carlo Approach to the Critical Properties of Self-Avoiding Random Walks.* Phys Rev B**27** 1635-1645

[2] Berg B and Foester D 1981 *Random Paths and Random Surfaces on a Digital Computer.* Phys Lett **106B** 323-326

[3] Burde G and Zieschang H 1985 *Knots.* De Gruyter Studies in Mathematics **5** (De Gruyter, Berlin)

[4] de Gennes P G 1979 *Scaling Concepts in Polymer Physics.* (Cornell University Press: New York)

[5] Delbrück M 1962 *Knotting Problems in Biology.* Proc Symp Appl Math **14** 55-63

[6] Diao Y 1993 *Minimal Knotted Polygons on the Cubic Lattice.* J. Knot Theo. Ram. **2** 413425

[7] Diao Y 1994 *The Number of Smallest Knots on the Cubic Lattice.* J. Stat. Phys. **74** 1247-1254

[8] Frisch H L and Wasserman E 1961 *Chemical Topology.* J Amer Chem Soc **83** 3789-3795

[9] Hammersley J M 1961 *The Number of Polygons on a Lattice.* Math Proc Camb Phil Soc **57** 516-523

[10] Janse van Rensburg E J 1999 *Minimal Lattice Knots.* Contributed to *Ideal Knots.* Series on Knots and Everything, Vol 19. Eds. A Stasiak, V Katritch and L H Kauffman (World Scientific, Singapore)

[11] Janse van Rensburg E J 2008 *Thoughts on Lattice Knot Statistics.* J Math Chem **45**(1) 7-38 (Commemorative issue in honour of S Whittington and R Kapral)

[12] Janse van Rensburg E J and Promislow S D 1995 *Minimal Knots in the Cubic Lattice.* J Knot Theo Ram **4** 115-130

[13] Janse van Rensburg E J and Rechnitzer A 2008 *Atmospheres of Polygons and Knotted Polygons.* J Phys A: Math Theo **41** 105002-25

[14] Janse van Rensburg E J and Rechnitzer A 2009 *Generalised Atmospheric Sampling of Self-Avoiding Walks.* J Phys A: Math Theo **42** 335001-30

[15] Janse van Rensburg E J and Rechnitzer A 2010 *Generalised Atmospheric Sampling of Knotted Polygons.* J Knot Theo Ram **20** 1145-71

[16] Janse van Rensburg E J and Rechnitzer A 2011 *BFACF-style Algorithms for Polygons in the Body-Centered and Face-Centered Cubic Lattices.* J Phys A: Math Theo **44** 165001

[17] Janse van Rensburg E J and Whittington S G 1991 *The BFACF Algorithm and Knotted Polygons.* J Phys A: Math Gen **24** 5553-5567

[18] Mann C, Mcloud-Mann J, Ranalli R and Smith N 2009 *Minimal Knotting Numbers.* J Knot Theo Ram **18** 1159-1173

[19] Michels J P J and Wiegel F W 1986 *On the Topology of a Polymer Ring.* Proc Roy Soc (London) A **403** 269-284

[20] Nishida N and Kaneko M 1959 *The apparent compressibility of high polymers in Solution.* J Fac Sci (Hokkaido University) Japan Ser II Vol V No 4 165-169

[21] Orlandini E, Tesi M C, Janse van Rensburg E J and Whittington S G 1998 *Asymptotics of Knotted Lattice Polygons.* J Phys A: Math Gen **31** 5953-5967

[22] Pippenger N 1989 *Knots in Self-Avoiding Walks.* Disc Appl Math **25** 273-278

[23] Portillo J, Diao Y, Scharein R, Arsuaga J and Vazquez M 2011 *On the Mean and Variance of the Writhe of Random Polygons.* J Phys A: Math Theo **44** 275004

[24] Rosenbluth M N and Rosenbluth A W 1955 *Monte Carlo Calculation of the Average Extension of Molecular Chains.* J Chem Phys **23** 356-359

[25] Scharein R, Ishihara K, Arsuaga J, Diao Y, Shimokawa K and Vazquez M 2009 *Bounds for Minimal Step Number of Knots in the Simple Cubic Lattice.* J Phys A: Math Theor **42** 475006

[26] Sumners D W and Whittington S G 1988 *Knots in Self-Avoiding Walks.* J Phys A: Math Gen **21** 1689-1694

[27] Vanderzande C 1995 *On Knots in a Model for the Adsorption of Ring Polymers.* J Phys A: Math Gen **28** 3681-3700

[28] Zhang W and Kiran E 2003 (p, V, T) *Behaviour and Miscibility of (Polysulfone+THF+Carbon Dioxide) at High Pressures.* J Chem Thermo **35** 605-624